Supplementary Information

Supplementary Methods 1. Processing and DNA extraction from tumor, peripheral blood mononuclear cells, and plasma samples

Supplementary Methods 2. Amplicon sequencing of primary tumor

Supplementary Methods 3. Identification of Somatic Mutation

Supplementary Methods 4. Amplicon sequencing of *TP53* gene in plasma DNA samples

Supplementary Methods 5. dPCR analysis

Supplementary Table S1. Clinicopathological characteristics of study patients

Supplementary Table S2. Target genes in the specifically designed SCC panel

Supplementary Table S3. Primary tumor mutations detected by sequencing analysis using the SCC panel

Supplementary Table S4. Treatment and outcomes of ESCC patients

Supplementary Table S5. Univariate analysis of overall survival for 34 ESCC patients

Supplementary Table S6. dPCR-evaluated mutations duplicatedly detected in multiple cases

Supplementary Figure S1. Flow chart of patient outcomes

Supplementary Figure S2. Blood sample collection processes

Supplementary Figure S3. ctDNA detection by digital PCR

Supplementary Figure S4. Variant allele frequencies of mutated genes in primary tumors

Supplementary Figure S5. Primary tumor-specific mutations and ctDNA in pretreatment plasma

Supplementary Figure S6. Correlation between VAFs measured by NGS and dPCR

Supplementary Figure S7. *NFE2L2* mutations in primary tumors and chemotherapeutic response

Supplementary Figure S8. Case presentations

Supplementary References

This supplementary material provides additional information about this study that was not included in the main text.

Supplementary Methods 1. Sample processing and DNA extraction from tumor, peripheral blood mononuclear cells, and plasma samples

Endoscopically acquired pretreatment primary tumor tissue and corresponding serial blood samples were obtained from all enrolled patients. In principle, the timing of imaging examinations, blood collection for ctDNA and serum tumor markers including squamous cell carcinoma antigen (SCC), carcinoembryonic antigen (CEA), and cytokeratin 19 fragments (CYFRA 21-1) were all intended to be matched.

Tumor tissues were stored at -80 °C until DNA extraction. Serial whole blood samples were collected into Cell-Free DNA Blood Collection Tubes (BCT®) (Streck, La Vista, NE) and stored at room temperature until plasma collection. To collect plasma samples, BCT tubes were centrifuged at 1800 × g for 20 min at room temperature using a swing-out rotor (KUBOTA, Tokyo, Japan). The plasma layer was transferred to a new 15 ml collection tube, and centrifuged at room temperature at 1800 × g for 20 min to remove any residual cellular debris. The supernatant was transferred again to a new cryotube and frozen at -80 °C until DNA extraction (supplementary Figure S2, top).

Peripheral blood mononuclear cells (PBMCs) were collected from the buffy coat layer after centrifugation of pretreatment whole blood samples in BCT tubes and were transferred into a BD Vacutainer® CPT™ Cell Preparation Tube (CPT) (supplementary

Figure S2, middle). According to this procedure, PBMCs can be isolated beyond the two-hour time window after blood collection in CPT, which avoids cytolytic release of cellular DNA from nucleated cells into the plasma (supplementary Figure S2, middle and bottom). Wollison et al. demonstrated by whole exome sequence and copy number microarray analyses that fixative in the BCT did not impact PBMC DNA quality [1]. In their sample collection procedure, plasma was stored after centrifugation of collected blood in BCT followed by DNA extraction from PBMC isolated from the remaining blood using a Gentra Puregene Blood Kit (Qiagen, Hilden, Germany). According to the kit protocol, several hours are required after centrifugation and removal of plasma to complete PBMC DNA extraction. Our combinatory method using both BCT and CPT for long-term preservation enables extraction of high-quality DNA from both plasma and PBMC after storage of up to seven days at room temperature. In this study, all plasma and PBMC samples were isolated within seven days of blood collection. Plasma DNA was extracted from 4-5 ml frozen plasma samples using a QIAamp® Circulating Nucleic Acid Kit according to the manufacturer's instructions (Qiagen, Hilden, Germany). Extracted DNA was eluted in 70-100 µl Qiagen Buffer AVE and stored at -20 °C until analysis. Tumor and PBMC DNA were isolated using a QIAamp® DNA Mini Kit (Qiagen, Hilden, Germany) and stored at -20 °C until analysis.

Supplementary Methods 2. Amplicon sequencing of primary tumors

For mutation screening of esophageal squamous cell cancer (ESCC) samples, a pair of tumor tissue samples and corresponding PBMCs was subjected to amplicon sequencing using the Ion PGM™ system according to the manufacturer's protocol (Thermo Fisher Scientific, Waltham, MA). Samples were sequenced using a specifically-designed SCC panel targeting 31 genes that have been reported to be frequently altered in ESCC and head and neck squamous cell carcinomas (supplementary Table S2) [2-8]. The SCC panel covers 617 exons of 31 genes and exon/intron boundaries with 1,194 amplicons. The entire length of the panel sequence is 220.57 kb, and the average amplicon size is 202 bp. Approximately 20 ng DNA per sample was used to prepare barcoded libraries with IonXpress barcoded adapters and an Ion AmpliSeq Library Kit 2.0 (Thermo Fisher Scientific). Ten individual barcoded libraries (100 pM each) were pooled and clonally amplified through emulsion PCR using a One Touch Instrument and the Ion PGM Template OT2 200 kit (Thermo Fisher Scientific). Finally, sequencing was performed on a PGM 316 chip using an Ion PGM 200 Sequencing Kit v2 according to the manufacturer's instructions (200 bp read length, Thermo Fisher Scientific). In this sequence analysis from primary ESCC tumor and PBMC DNA, the average base

coverage depth was 2,864 and the average percent reads on target was 91.8%.

Supplementary Methods 3. Identification of somatic mutations

Genome Reference Consortium Human Build 37 (GRCh37/hg19) was used as a reference. Alignment to the GRCh37/hg19 genome and sequencing read counting were performed in Torrent Suite version 5.0 (Thermo Fisher Scientific). Somatic mutations, including single-nucleotide variants, insertions, and deletions were detected using a variant call algorithm in tumor- and matched-PBMC samples from the Ion Reporter software 5.0 tumor-normal workflow (Thermo Fisher Scientific), in which germline variants were subtracted from the tumor variants as previously described [9]. All identified single-nucleotide variants (SNVs), insertions, and deletions (INDELs) were visually inspected using Integrative Genomics Viewer software to filter out possible strand-specific errors, such as a mutation detected in only the forward or reverse DNA strand. The dbSNP database was used to exclude single nucleotide polymorphisms (SNPs) from the called variants. The following criteria were used as cutoffs: (i) total coverage >200, (ii) variant coverage >6, and (iii) variant frequency >2%. Mutations were called if they occurred in <0.1% of reads in the normal control (minor allele frequency) and were absent from dbSNP as well as the 1000 Genomes Project database.

Supplementary Methods 4. Amplicon sequencing of *TP53* gene in plasma DNA samples

For mutation screening, plasma DNA samples from 28 patients with Stage IB or higher disease were subjected to amplicon sequencing using an Ion AmpliSeq™ *TP53* Panel according to the manufacturer's protocol (Thermo Fisher Scientific). This 1,280 bp panel has 24 amplicons that cover all coding exons of the *TP53* gene and produces an average amplicon size of 106 bp.

Supplementary Methods 5. dPCR analysis

PCR reactions were prepared with 7.5 µl QuantStudio3D Digital PCR master mix (Thermo Fisher Scientific), 1.5 µL primer/probe mix for each mutation (adjusted to a final concentration of 900 nM of forward and reverse primers and 250 nM for wild type and mutant probes) and plasma or tumor DNA (3-20 ng) in a total volume of 15 µl. PCR products were loaded onto a QuantStudio 3D Digital PCR Chip (Thermo Fisher Scientific) and amplified using the ProFlex 2x Flat PCR System (Thermo Fisher Scientific). The annealing and extension temperatures were set at 56 °C or 60 °C, and PCR was run for 39 cycles. After PCR amplification, chips were read on a QuantStudio

3D Digital PCR Instrument (Thermo Fisher Scientific), and a secondary analysis was performed with QuantStudio 3D Analysis Suit Cloud software (Thermo Fisher Scientific). For further quality control, the boundaries of FAM, VIC, and undetermined events can be manually defined.

After confirmation of sufficiently separate reactions of both wild type and mutant alleles in tumor DNA, plasma DNA was evaluated by dPCR (supplementary Figure S3A). Plasma samples having more than two positive reactions (i.e., dots) for mutant DNA were defined as ctDNA-positive samples. If only one positive reaction for mutant DNA was detected, samples meeting the following criteria were considered as ctDNA-positive: (i) more than one positive reaction for mutant DNA could be repeatedly detected upon retesting the same sample; (ii) more than one positive reaction for the same mutant DNA was detected in samples collected at similar time points; (iii) more than one positive reaction for another mutant DNA was detected in the same sample (supplementary Figure S3B). The VAF values were calculated as the fraction of mutant/(mutant + wild) divided by the number of partitions in which either the mutant or wild-type sequence was detected [10]. If no mutant partitions were detected, the case DNA was regarded as "negative".

Supplementary References

1. Wollison BM, Thai E, McKinney A et al. Blood collection in cell-stabilizing tubes does not impact germline DNA quality for pediatric patients. PLoS One 2017; 12: e0188835.

2. Gao YB, Chen ZL, Li JG et al. Genetic landscape of esophageal squamous cell carcinoma. Nat Genet 2014; 46: 1097-1102.

3. Lin DC, Hao JJ, Nagata Y et al. Genomic and molecular characterization of esophageal squamous cell carcinoma. Nat Genet 2014; 46: 467-473.

4. Song Y, Li L, Ou Y et al. Identification of genomic alterations in oesophageal squamous cell cancer. Nature 2014; 509: 91-95.

5. Sawada G, Niida A, Uchi R et al. Genomic landscape of esophageal squamous cell carcinoma in a japanese population. Gastroenterology 2016; 150: 1171-1182.

6. Agrawal N, Frederick MJ, Pickering CR et al. Exome sequencing of head and neck squamous cell carcinoma reveals inactivating mutations in NOTCH1. Science 2011; 333: 1154-1157.

7. Stransky N, Egloff AM, Tward AD et al. The mutational landscape of head and neck squamous cell carcinoma. Science 2011; 333: 1157-1160.

8. Pickering CR, Zhang J, Yoo SY et al. Integrative genomic characterization of

oral squamous cell carcinoma identifies frequent somatic drivers. Cancer Discov 2013; 3: 770-781.

9. Nakagaki T, Tamura M, Kobashi K et al. Profiling cancer-related gene mutations in oral squamous cell carcinoma from Japanese patients by targeted amplicon sequencing. Oncotarget 2017; 8: 59113-59122.

10. Huggett JF, Foy CA, Benes V et al. The digital MIQE guidelines: Minimum information for publication of quantitative digital PCR experiments. Clin Chem 2013; 59: 892-902.

Supplementary Table S1. Clinicopathological characteristics of study patients

Patient ID	Age	Gender	Locus [a]	UICC stage [b]	TNM [b]	pretreatment tumor volume (cm^3)
EC_1	67	Male	Ut	IIIA	T1bN2M0	0.8
EC_2	66	Male	LtAeG	IIIC	T4bN1M0	521.8
EC_3	69	Male	LtAe	IV	T3N2M1	142.8
EC_4	65	Male	CeUt	IIIC	T4bN1M0	16.2
EC_5	60	Female	Ae	IA	T1bN0M0	1.1
EC_6	56	Male	Ut	IIA	T3N0M0	6.6
EC_7	62	Female	MtUt	IIIA	T3N1M0	15.6
EC_8	67	Male	MtUtLt	IIIC	T4bN2M0	78.9
EC_9	81	Male	MtLtAe	IIIB	T3N2M0	25.8
EC_10	71	Female	Mt	IIIC	T4bN1M0	32.9
EC_11	71	Female	MtUtLt	IV	T3N3M1	247.4
EC_12	76	Male	Mt	IA	T1bN0M0	0.1
EC_13	81	Male	Lt	IV	T3N1M1	21.9
EC_14	65	Male	UtMt	IIIC	T4bN2M0	59.5
EC_15	78	Male	MtLt	IV	T4bN2M1	79.7
EC_16	55	Female	Lt	IIIB	T3N2M0	17.3
EC_17	75	Female	Ae	IIIA	T3N1M0	12.6
EC_18	78	Male	Lt	IV	T1bN2M1	14.2
EC_19	70	Male	LtAe	IIIC	T4bN1M0	64.1
EC_20	57	Male	Ae	IIIA	T3N1M0	68.7
EC_21	48	Male	Lt	IIA	T3N0M0	22.6
EC_22	75	Male	Mt	IIB	T2N1M0	3.8
EC_23	77	Male	Mt	IA	T1bN0M0	0.5
EC_24	53	Male	UtMt	IIIC	T4bN0M0	35.3
EC_25	74	Male	Lt	IIIA	T3N1M0	9.4
EC_26	63	Male	Mt	IIIC	T4bN1M0	37.5
EC_27	68	Male	Mt	IA	T1aN0M0	1.3
EC_28	78	Male	Mt	IA	T1bN0M0	0.2
EC_29	65	Male	Mt	IIIC	T4bN2M0	30.9
EC_30	65	Male	LtMt	IIIB	T3N2M0	81.6
EC_31	77	Male	Ut	IA	T1aN0M0	0.2
EC_32	66	Female	LtMt	IIIC	T4aN1M0	44.9
EC_33	80	Male	Ut	IIIC	T4bN1M0	24.9
EC_34	73	Male	Lt	IA	T1bN0M0	1.8
EC_35	64	Male	Mt	IIIC	T4bN3M0	56.6
EC_36	64	Male	Ut	IB	T2N0M0	4.5

[a] Anatomical regions of the esophagus: Ce, Cervical esophagus; Ut, Upper thoracic esophagus; Mt, Middle thoracic esophagus; Lt, Lower thoracic esophagus; Ae, Abdominal esophagus (Japanese Classification of Esophageal Cancer, 11th edition)
[b] TNM classification, 7th edition

Supplementary Table S2. Target genes in the specifically designed SCC panel

AJUBA	*CASP8*	*CCND1*	*CDKN2A*	*CREBBP*
EGFR	*EP300*	*FAT1*	*FAT2*	*FBXW7*
FGFR1	*HRAS*	*KDM6A*	*KEAP1*	*KMT2C*
KMT2D	*NFE2L2*	*NOTCH1*	*NOTCH2*	*NOTCH3*
NSD1	*PIK3CA*	*PTEN*	*RB1*	*SOX2*
TET2	*TGFBR2*	*TP53*	*TP63*	*YAP1*
ZNF750				

Supplementary Table S3. Primary tumor mutations detected by sequencing analysis using the SCC panel

Case ID	Chromosomal location	gene	Variant type	Base change	Amino acid change	Total allele	Normal allele	Variant allele	VAF[a] (%)	dPCR [b]
EC_1	chr4:153249422	*FBXW7*	missense	c.1356A>T	p.Glu452Asp	1743	1430	313	18.0	
	chr16:3781366	*CREBBP*	missense	c.4999T>C	p.Phe1667Leu	909	880	29	3.2	
	chr17:7578394	*TP53*	missense	c.536A>G	p.His179Arg	1989	1500	489	24.6	Yes
	chr17:80789877	*ZNF750*	frameshiftDeletion	c.453_453delT	p.Ala152fs	1994	1394	600	30.1	Yes
	chr19:15299961	*NOTCH3*	missense	c.1217G>A	p.Gly406Asp	1495	1319	176	11.8	
	chr17:7576845	*TP53*	intron	c.993+8G>T		1997	1678	319	16.0	
	chr2:178095689	*NFE2L2*	missense	c.1642A>G	p.Lys548Glu	911	881	30	3.3	
	chr2:178095693	*NFE2L2*	missense	c.1638T>G	p.Asn546Lys	902	862	40	4.4	
	chr7:55238875	*EGFR*	missense	c.1888G>A	p.Gly630Arg	1377	1339	38	2.8	
	chr7:151945007	*KMT2C*	missense	c.2512G>A	p.Gly838Ser	1233	1151	82	6.7	
	chr7:151962265	*KMT2C*	missense	c.1042G>A	p.Asp348Asn	1278	1228	50	3.9	
	chr12:49426896	*KMT2D*	missense	c.11592C>G	p.His3864Gln	2000	1889	111	5.6	
	chr12:49445055	*KMT2D*	missense	c.2411T>C	p.Leu804Ser	983	919	64	6.5	
	chr16:3779323	*CREBBP*	missense	c.5725C>A	p.Pro1909Thr	1999	1929	70	3.5	
EC_2	chr4:187549359	*FAT1*	missense	c.4759C>G	p.Leu1587Val	2000	1232	768	38.4	
	chr8:38279361	*FGFR1*	missense	c.1128C>G	p.Asn376Lys	1995	1082	913	45.8	Yes
	chr17:7578235	*TP53*	missense	c.614A>G	p.Tyr205Cys	1999	1242	757	37.9	Yes
	chr17:7578271	*TP53*	missense	c.578A>G	p.His193Arg	2000	1713	287	14.4	Yes
	chr3:178927381	*PIK3CA*	splicesite	c.1146-2A>G		1999	1,643	356	17.8	
	chr7:151945007	*KMT2C*	missense	c.2512G>A	p.Gly838Ser	1999	1913	86	4.3	
EC_3	chr2:178098799	*NFE2L2*	missense	c.246A>T	p.Glu82Asp	1131	665	466	41.2	Yes
	chr4:187629603	*FAT1*	missense	c.1379C>A	p.Pro460His	1984	1911	73	3.7	
	chr7:151859911	*KMT2C*	missense	c.10751G>T	p.Gly3584Val	1876	1775	101	5.4	
	chr7:151921670	*KMT2C*	missense	c.3008G>A	p.Arg1003Lys	1237	1162	75	6.1	
	chr17:7578431	*TP53*	nonsense	c.499C>T	p.Gln167Ter	277	118	159	57.4	Yes
	chr4:106155506	*TET2*	missense	c.407G>A	p.Ser136Asn	745	710	35	4.7	
	chr7:55219001	*EGFR*	missense	c.574C>T	p.Pro192Ser	1994	1842	152	7.6	
	chr7:151970856	*KMT2C*	missense	c.946A>T	p.Thr316Ser	1591	1459	132	8.3	
	chr12:49426896	*KMT2D*	missense	c.11592C>G	p.His3864Gln	1999	1925	74	3.7	
	chr12:49445055	*KMT2D*	missense	c.2411T>C	p.Leu804Ser	1126	1049	77	6.8	
	chr16:3779323	*CREBBP*	missense	c.5725C>A	p.Pro1909Thr	1996	1878	118	5.9	
EC_4	chr2:178098799	*NFE2L2*	missense	c.246A>T	p.Glu82Asp	1322	875	447	33.8	Yes
	chr13:48916851	*RB1*	splicesite	c.381+1G>T		1546	857	689	44.6	
	chr5:150924318	*FAT2*	missense	c.6370G>A	p.Asp2124Asn	2000	1925	75	3.8	
	chr5:176636829	*NSD1*	missense	c.1429A>G	p.Lys477Glu	1999	1939	60	3.0	
	chr7:151860616	*KMT2C*	missense	c.10046C>T	p.Pro3349Leu	1186	1130	56	4.7	
	chr12:49426644	*KMT2D*	missense	c.11843_11844delTTinsAA	p.Leu3948Gln	623	598	25	4.0	
	chr17:7578190	*TP53*	missense	c.659A>G	p.Tyr220Cys	1996	633	1363	68.3	Yes
	chr1:120465015	*NOTCH2*	missense	c.5057T>C	p.Val1686Ala	2000	1930	70	3.5	
	chr7:151945007	*KMT2C*	missense	c.2512G>A	p.Gly838Ser	779	719	60	7.7	
	chr12:49445055	*KMT2D*	missense	c.2411T>C	p.Leu804Ser	660	619	41	6.2	
EC_5	chr9:139418261	*NOTCH1*	missense	c.311A>C	p.Asn104Thr	2000	1923	77	3.9	
	chr16:3778807	*CREBBP*	nonsense	c.6241C>T	p.Gln2081Ter	1295	1172	123	9.5	
	chr16:3786715	*CREBBP*	missense	c.4496T>C	p.Leu1499Pro	2000	1801	199	10.0	
	chr16:3807844	*CREBBP*	missense	c.3575T>G	p.Val1192Gly	1992	1906	86	4.3	
	chr16:3828817	*CREBBP*	missense	c.1825G>A	p.Val609Ile	1812	1652	160	8.8	
	chr17:7578212	*TP53*	nonsense	c.637C>T	p.Arg213Ter	1993	1704	289	14.5	Yes
	chr19:15298716	*NOTCH3*	missense	c.1582G>T	p.Gly528Cys	1997	1797	200	10.0	
EC_6	chr7:151927023	*KMT2C*	nonsense	c.2961C>G	p.Tyr987Ter	220	205	15	6.8	
	chr7:151945256	*KMT2C*	nonsense	c.2263C>T	p.Gln755Ter	1999	1924	75	3.8	
	chr12:49445055	*KMT2D*	missense	c.2411T>C	p.Leu804Ser	397	371	26	6.5	
	chr14:23451144	*AJUBA*	frameshiftInsertion	c.331_332insGC	p.Leu111fs	1995	1316	679	34.0	Yes
	chr16:3779323	*CREBBP*	missense	c.5725C>A	p.Pro1909Thr	1999	1942	57	2.9	
	chr17:7578190	*TP53*	missense	c.659A>G	p.Tyr220Cys	1997	1115	882	44.2	Yes
	chr19:10602620	*KEAP1*	missense	c.958C>T	p.Arg320Trp	1999	1892	107	5.4	
EC_7	chr7:151945007	*KMT2C*	missense	c.2512G>A	p.Gly838Ser	1854	1699	155	8.4	
	chr17:7577500	*TP53*	frameshiftDeletion	c.780_780delC	p.Ser260fs	1990	1407	583	29.3	Yes
	chr19:15292506	*NOTCH3*	nonsense	c.2673C>A	p.Cys891Ter	845	625	220	26.0	Yes
EC_8	chr4:187629772	*FAT1*	missense	c.1210A>G	p.Ser404Gly	1994	1920	74	3.7	
	chr7:151945256	*KMT2C*	nonsense	c.2263C>T	p.Gln755Ter	1997	1903	94	4.7	
	chr16:3842089	*CREBBP*	missense	c.1223A>G	p.His408Arg	1137	974	163	14.3	
	chr17:7578235	*TP53*	missense	c.614A>G	p.Tyr205Cys	1999	1473	526	26.3	Yes
	chr22:41565575	*EP300*	missense	c.4241A>G	p.Tyr1414Cys	1232	928	304	24.7	
EC_9	chr3:181431028	*SOX2*	|missense	c.880A>G	|p.Met294Val	369	355	14	3.8	
	chr3:189604293	*TP63*	missense	c.1460G>A	p.Arg487His	1983	1726	257	13.0	
	chr4:187629772	*FAT1*	missense	c.1210A>G	p.Ser404Gly	1997	1925	72	3.6	
	chr9:139412278	*NOTCH1*	missense	c.1367G>A	p.Cys456Tyr	1999	1917	82	4.1	
	chr12:49445055	*KMT2D*	missense	c.2411T>C	p.Leu804Ser	463	425	38	8.2	
	chr14:23451000	*AJUBA*	frameshiftInsertion	c.475_476insA	p.Ser159fs	1989	1424	565	28.4	Yes
	chr16:3779323	*CREBBP*	missense	c.5725C>A	p.Pro1909Thr	1999	1936	63	3.2	
	chr17:7578455	*TP53*	missense	c.475G>C	p.Ala159Pro	202	159	43	21.3	Yes
EC_10	chr1:120471716	*NOTCH2*	nonsense	c.3775G>T	p.Glu1259Ter	1991	1804	187	9.4	
	chr5:150907682	*FAT2*	missense	c.10039G>A	p.Asp3347Asn	1991	1610	381	19.1	Yes
	chr9:139413049	*NOTCH1*	missense	c.1093C>T	p.Arg365Cys	2000	1959	41	2.1	
	chr14:23450825	*AJUBA*	frameshiftInsertion	c.650_651insCA	p.Gln217fs	1991	1204	787	39.5	Yes
	chr16:3779323	*CREBBP*	missense	c.5725C>A	p.Pro1909Thr	1921	1858	63	3.3	

	chr16:3807844	*CREBBP*	missense	c.3575T>G	p.Val1192Gly	1994	1922	72	3.6	
	chr17:7578370	*TP53*	splicesite	c.559+1C>T		1999	1378	621	31.1	Yes
EC_11	chr17:7577556	*TP53*	missense	c.725G>T	p.Cys242Phe	1988	1343	645	32.4	Yes
	chr7:151945007	*KMT2C*	missense	c.2512G>A	p.Gly838Ser	2000	1876	124	6.2	
	chr7:151970856	*KMT2C*	missense	c.946A>T	p.Thr316Ser	1998	1837	161	8.1	
	chr12:49445055	*KMT2D*	missense	c.2411T>C	p.Leu804Ser	848	790	58	6.8	
EC_12	chr2:178098965	*NFE2L2*	missense	c.80A>G	p.Asp27Gly	1994	1381	613	30.7	
	chr17:7577530	*TP53*	frameshiftDeletion	c.750_750delC	p.Ile251fs	1995	1951	44	2.2	
	chr17:7577574	*TP53*	missense	c.707A>G	p.Tyr236Cys	1999	809	1190	59.5	Yes
	chr3:181431028	*SOX2*	missense	c.880A>G	p.Met294Val	209	200	9	4.3	
	chr12:49445055	*KMT2D*	missense	c.2411T>C	p.Leu804Ser	390	356	34	8.7	
	chr16:3779323	*CREBBP*	missense	c.5725C>A	p.Pro1909Thr	890	852	38	4.3	
EC_13	chr3:181431028	*SOX2*	missense	c.880A>G	p.Met294Val	260	252	8	3.1	
	chr17:7579358	*TP53*	missense	c.329G>T	p.Arg110Leu	1766	1447	319	18.1	Yes
	chr17:80788479	*ZNF750*	|nonsense	c.1711C>T	p.Arg571Ter	1673	1357	316	18.9	
	chr7:151945007	*KMT2C*	missense	c.2512G>A	p.Gly838Ser	1614	1505	109	6.8	
	chr12:49445055	*KMT2D*	missense	c.2411T>C	p.Leu804Ser	224	212	12	5.4	
	chr16:3807844	*CREBBP*	missense	c.3575T>G	p.Val1192Gly	1993	1939	54	2.7	
EC_14	chr2:178095691	*NFE2L2*	missense	c.1640A>G	p.Asp547Gly	1999	1341	658	32.9	
	chr2:178098809	*NFE2L2*	missense	c.236A>C	p.Glu79Ala	1995	1352	643	32.2	
	chr14:23447575	*AJUBA*	frameshiftInsertion	c.1085_1086insTGGACAGCCTCTACCACACCCA	p.Gln362fs	1975	795	1180	59.7	
	chr16:3777761	*CREBBP*	missense	c.7285_7287delGACinsACG	p.Asp2429Thr	1995	1931	64	3.2	
	chr17:7578550	*TP53*	missense	c.380C>T	p.Ser127Phe	209	68	141	67.5	Yes
	chr12:49434075	*KMT2D*	missense	c.7478G>T	p.Gly2493Val	1049	1013	36	3.4	
EC_15	chr17:7577120	*TP53*	missense	c.818G>A	p.Arg273His	1170	461	708	60.5	Yes
	chr14:23450675	*AJUBA*	frameshiftInsertion	c.800_801insTA	p.Gly268fs	1766	697	974	55.2	Yes
	chr9:21971035	*CDKN2A*	frameshiftDeletion	c.310_322delCTGGACGTGCGCG	p.Leu104fs	1857	1040	817	44.0	Yes
	chr2:178098815	*NFE2L2*	missense	c.230A>T	p.Asp77Val	1277	1239	38	3.0	
	chr4:106157845	*TET2*	nonsense	c.2746C>T	p.Gln916Ter	1241	1116	125	10.1	
	chr9:139401755	*NOTCH1*	frameshiftDeletion	c.3633_3644+1delCCCTGAGTGCCC	p.Arg1211fs	1791	823	42	2.3	
EC_16	chr17:7578271	*TP53*	missense	c.578A>T	p.His193Leu	1998	551	1447	72.4	Yes
	chr2:178098806	*NFE2L2*	missense	c.239C>A	p.Thr80Lys	1735	789	946	54.5	Yes
	chr4:153247289	*FBXW7*	missense	c.1513C>G	p.Arg505Gly	1255	1229	26	2.1	
	chr7:151945256	*KMT2C*	nonsense	c.2263C>T	p.Gln755Ter	1998	1814	184	9.2	
	chr10:89692985	*PTEN*	missense	c.469G>A	p.Glu157Lys	547	511	36	6.6	
	chr12:49445055	*KMT2D*	missense	c.2411T>C	p.Leu804Ser	269	253	16	5.9	
	chr16:3807844	*CREBBP*	missense	c.3575T>G	p.Val1192Gly	1969	1875	94	4.8	
EC_17	chr17:7577551	*TP53*	missense	c.730G>A	p.Gly244Ser	2000	1815	185	9.3	Yes[d]
	chr7:151945007	*KMT2C*	missense	c.2512G>A	p.Gly838Ser	1999	1828	171	8.6	
	chr12:49445055	*KMT2D*	missense	c.2411T>C	p.Leu804Ser	984	935	49	5.0	
	chr12:49426669	*KMT2D*	missense	c.11819T>A	p.Leu3940His	372	357	15	4.0	
	chr16:3807844	*CREBBP*	missense	c.3575T>G	p.Val1192Gly	1989	1924	65	3.3	
EC_18	chr17:7578235	*TP53*	missense	c.614A>G	p.Tyr205Cys	2000	1719	281	14.1	Yes
	chr9:139413094	*NOTCH1*	missense	c.1048T>C	p.Cys350Arg	1996	1886	110	5.5	
	chr9:139391555	*NOTCH1*	missense	c.6636C>A	p.Asp2212Glu	1999	1408	591	29.6	Yes
	chr7:151945228	*KMT2C*	missense	c.2291C>T	p.Ser764Phe	2000	1812	188	9.4	
EC_19	chr1:120539833	*NOTCH2*	missense	c.538G>A	p.Glu180Lys	1999	1870	362	18.1	
	chr2:178098799	*NFE2L2*	missense	c.246A>T	p.Glu82Asp	1990	1521	469	23.6	Yes
	chr7:151900060	*KMT2C*	missense	c.4051A>G	p.Arg1351Gly	1974	376	129	6.5	
	chr9:139412303	*NOTCH1*	nonsense	c.1342C>T	p.Arg448Ter	1989	1400	589	29.6	Yes
	chr17:7578526	*TP53*	frameshiftInsertion	c.399_400insCAAGATG	p.Phe134fs	207	127	80	38.6	Yes
	chr12:49445046	*KMT2D*	missense	c.2420C>G	p.Ser807Cys	391	173	74	18.9	
EC_20	chr12:49445055	*KMT2D*	missense	c.2411T>C	p.Leu804Ser	1136	1073	63	5.5	
EC_21	chr17:7578190	*TP53*	missense	c.659A>G	p.Tyr220Cys	1471	1025	446	30.3	Yes
	chr9:21974786	*CDKN2A*	frameshiftDeletion	c.40delG	p.Asp14fs	132	109	23	17.4	Yes[c]
	chr9:139412297	*NOTCH1*	missense	c.1348G>A	p.Glu450Lys	2000	1859	141	7.1	
	chr17:7577099	*TP53*	missense	c.839G>C	p.Arg280Thr	1999	1829	170	8.5	Yes[d]
	chr4:187538943	*FAT1*	nonsense	c.8797C>T	p.Gln2933Ter	1999	1927	72	3.6	
	chr4:187560876	*FAT1*	missense	c.3641_3642delAGinsTA	p.Glu1214Val	1999	1936	63	3.2	
	chr7:151945256	*KMT2C*	nonsense	c.2263C>T	p.Gln755Ter	1999	1875	124	6.2	
	chr12:49445055	*KMT2D*	missense	c.2411T>C	p.Leu804Ser	936	894	42	4.5	
	chr17:7579473	*TP53*	missense	c.214C>G	p.Pro72Ala	1999	1930	69	3.5	
EC_22	chr17:7578403	*TP53*	missense	c.527G>A	p.Cys176Tyr	1997	1418	579	29.0	Yes
	chr7:151927023	*KMT2C*	nonsense	c.2961C>G	p.Tyr987Ter	207	189	18	8.7	
	chr7:151927067	*KMT2C*	missense	c.2917A>G	p.Arg973Gly	223	204	19	8.5	
	chr7:151945256	*KMT2C*	nonsense	c.2263C>T	p.Gln755Ter	2000	1845	155	7.8	
	chr12:49426669	*KMT2D*	missense	c.11819T>A	p.Leu3940His	355	336	19	5.4	
	chr12:49445055	*KMT2D*	missense	c.2411T>C	p.Leu804Ser	622	580	42	6.8	
	chr17:7579473	*TP53*	missense	c.214C>G	p.Pro72Ala	2000	1876	124	6.2	
EC_23	chr2:202131352	*CASP8*	missense	c.320T>G	p.Leu107Arg	1988	1374	614	30.9	
	chr2:178098960	*NFE2L2*	missense	c.85G>A	p.Asp29Asn	1981	1327	654	33.0	
	chr17:7577129	*TP53*	missense	c.809T>G	p.Phe270Cys	1998	1329	669	33.5	Yes
	chr17:7577534	*TP53*	missense	c.747G>T	p.Arg249Ser	1999	1377	622	31.1	
	chr7:151945007	*KMT2C*	missense	c.2512G>A	p.Gly838Ser	1457	1364	93	6.4	
EC_24	chr17:7579389	*TP53*	nonsense	c.298C>T	p.Gln100Ter	1119	507	612	54.7	Yes
	chr1:120464356	*NOTCH2*	missense	c.5290C>A	p.Pro1764Thr	441	406	35	7.9	
	chr7:55219001	*EGFR*	missense	c.574C>T	p.Pro192Ser	762	709	53	7.0	
	chr5:150905399	*FAT2*	missense	c.10436C>A	p.Pro3479Gln	521	486	35	6.7	
	chr12:49445055	*KMT2D*	missense	c.2411T>C	p.Leu804Ser	226	211	15	6.6	
	chr4:187628886	*FAT1*	missense	c.2096T>A	p.Val699Glu	550	529	21	3.8	
	chr9:139396800	*NOTCH1*	missense	c.5308C>T	p.Pro1770Ser	224	216	8	3.6	

	chr2:202139654	*CASP8*	missense	c.815G>A	p.Arg272Lys	227	219	8	3.5	
	chr2:202137660	*CASP8*	nonsense	c.767C>A	p.Ser256Ter	475	459	16	3.4	
	chr22:41548280	*EP300*	missense	c.3068T>A	p.Ile1023Lys	390	378	12	3.1	
	chr4:106158099	*TET2*	missense	c.3000C>A	p.Asn1000Lys	1416	1382	34	2.4	
EC_25	chr4:106156736	*TET2*	missense	c.1637A>C	p.Lys546Thr	294	287	7	2.4	
	chr4:153244137	*FBXW7*	missense	c.2020C>T	p.Arg674Trp	317	305	12	3.8	
	chr4:187509910	*FAT1*	missense	c.13603A>T	p.Met4535Leu	1630	1578	52	3.2	
	chr5:150922608	*FAT2*	missense	c.8080C>G	p.Pro2694Ala	214	207	7	3.3	
	chr5:176636829	*NSD1*	missense	c.1429A>G	p.Lys477Glu	1277	1248	29	2.3	
	chr7:151836843	*KMT2C*	missense	c.14377A>C	p.Lys4793Gln	386	367	19	4.9	
	chr7:151860431	*KMT2C*	missense	c.10231C>G	p.Gln3411Glu	233	223	10	4.3	
	chr7:151962265	*KMT2C*	missense	c.1042G>A	p.Asp348Asn	690	672	18	2.6	
	chr9:139412281	*NOTCH1*	missense	c.1364A>T	p.Glu455Val	949	911	38	4.0	
	chr9:139412609	*NOTCH1*	missense	c.1235A>T	p.Asp412Val	1350	1309	41	3.0	
	chr12:49445055	*KMT2D*	missense	c.2411T>C	p.Leu804Ser	223	214	9	4.0	
	chr17:7577545	*TP53*	missense	c.736A>T	p.Met246Leu	1999	1935	64	3.2	Yes[d]
EC_26	chr1:120464356	*NOTCH2*	missense	c.5290C>A	p.Pro1764Thr	322	297	25	7.8	
	chr3:189349366	*TP63*	missense	c.62G>C	p.Arg21Pro	468	452	16	3.4	
	chr4:187560876	*FAT1*	missense	c.3641_3642delAGinsTA	p.Glu1214Val	281	270	11	3.9	
	chr4:187628886	*FAT1*	missense	c.2096T>A	p.Val699Glu	644	614	30	4.7	
	chr5:150924318	*FAT2*	missense	c.6370G>A	p.Asp2124Asn	627	611	16	2.6	
	chr5:176636829	*NSD1*	missense	c.1429A>G	p.Lys477Glu	800	752	48	6.0	
	chr7:55238875	*EGFR*	missense	c.1888G>A	p.Gly630Arg	319	308	11	3.4	
	chr7:151860616	*KMT2C*	missense	c.10046C>T	p.Pro3349Leu	259	244	15	5.8	
	chr7:151879637	*KMT2C*	missense	c.5308A>G	p.Thr1770Ala	222	216	6	2.7	
	chr7:151945256	*KMT2C*	nonsense	c.2263C>T	p.Gln755Ter	1003	940	63	6.3	
	chr7:151962265	*KMT2C*	missense	c.1042G>A	p.Asp348Asn	473	457	16	3.4	
	chr9:139412278	*NOTCH1*	missense	c.1367G>A	p.Cys456Tyr	1209	1150	59	4.9	
	chr9:139412326	*NOTCH1*	missense	c.1319G>T	p.Cys440Phe	1277	1225	52	4.1	
	chr9:139412676	*NOTCH1*	missense	c.1168A>G	p.Asn390Asp	1607	1514	93	5.8	
	chr9:139412690	*NOTCH1*	missense	c.1154C>A	p.Ser385Tyr	1575	1481	94	6.0	
	chr9:139418261	*NOTCH1*	missense	c.311A>C	p.Asn104Thr	1254	1195	59	4.7	
	chr11:69466021	*CCND1*	missense	c.859C>A	p.Pro287Thr	836	805	31	3.7	
	chr16:3781885	*CREBBP*	missense	c.4782C>G	p.Asn1594Lys	432	423	9	2.1	
	chr17:7577094	*TP53*	missense	c.844C>T	p.Arg282Trp	283	277	6	2.1	Yes[d]
	chrX:44929089	*KDM6A*	missense	c.2189C>A	p.Thr730Lys	715	694	21	2.9	
EC_28	chr1:120479954	*NOTCH2*	missense	c.3473G>A	p.Cys1158Tyr	858	534	324	37.8	
	chr2:178098949	*NFE2L2*	In-frameDeletion	c.69_95delTTGGAGGCAAGATATAGATCTTGGAGT	p.Trp24_Val32del	374	204	170	45.5	
	chr11:69456241	*CCND1*	missense	c.160C>T	p.Pro54Ser	1210	917	293	24.2	
	chr17:7577551	*TP53*	missense	c.730G>A	p.Gly244Ser	1367	414	949	69.4	Yes
EC_29	chr17:7577104	*TP53*	missense	c.832C>T	p.Pro278Ser	1447	1203	241	16.7	Yes
	chr17:80789818	*ZNF750*	frameshiftDeletion	c.512delA	p.Lys171fs	1989	1538	451	22.7	
EC_30	chr17:7577094	*TP53*	missense	c.844C>T	p.Arg282Trp	989	588	401	40.5	Yes
	chr17:7578256	*TP53*	missense	c.578A>G	p.His193Arg	1959	1241	707	36.1	Yes
	chrX:44938585	*KDM6A*	nonsense	c.3133G>T	p.Glu1045Ter	590	56	534	90.5	
EC_31	chr4:153244184	*FBXW7*	missense	c.1973G>A	p.Arg658Gln	864	585	279	32.3	
	chr17:7577498	*TP53*	splicesite_	c.782+1G>A		1999	1063	936	46.8	Yes
EC_32	chr4:187629395	*FAT1*	frameshiftDeletion	c.1586delT	p.Leu529fs	1347	1121	226	16.8	
	chr4:187630547	*FAT1*	missense	c.435G>C	p.Leu145Phe	1430	1023	407	28.5	
	chr7:151842343	*KMT2C*	missense	c.14069G>A	p.Arg4690Gln	1068	835	233	21.8	
	chr9:21971036	*CDKN2A*	missense	c.322G>C	p.Asp108His	866	537	329	38.0	
	chr17:7577518	*TP53*	missense|missense	c.760_763delATCAinsTTCT	p.Ile254_Ile255delinsPhePhe	1984	1532	446	22.5	Yes
	chr17:7579315	*TP53*	frameshiftInsertion	c.371_372insTG	p.Thr125fs	1971	1512	459	23.3	Yes
	chr17:80788986	*ZNF750*	nonsense	c.1345G>T	p.Glu449Ter	1355	771	584	43.1	
	chr19:10602845	*KEAP1*	missense	c.733G>T	p.Val245Phe	1999	1389	610	30.5	Yes
EC_33	chr17:7578231	*TP53*	missense	c.614A>G	p.Tyr205Cys	1989	1865	123	6.2	Yes[d]
	chr17:7579356	*TP53*	missense	c.331C>A	p.Leu111Met	1993	1846	147	7.4	Yes[d]
EC_34	chr7:151878992	*KMT2C*	missense	c.5953T>G	p.Ser1985Ala	819	248	571	69.7	
	chr7:151945204	*KMT2C*	missense	c.2315C>T	p.Ser772Leu	1621	646	975	60.1	
	chr17:7578291	*TP53*	splicesite	c.560-2A>G		2000	359	1635	81.8	Yes
EC_35	chr17:7577528	*TP53*	missense	c.743G>A	p.Arg248Gln	1992	1831	112	5.6	Yes[d]
EC_36	chr2:178098959	*NFE2L2*	missense	c.86A>G	p.Asp29Gly	2000	1477	523	26.2	Yes
	chr17:7578190	*TP53*	missense	c.659A>G	p.Tyr220Cys	1560	846	714	45.8	Yes
	chr17:7578371	*TP53*	missense	c.559 G>C	p.Gly187Arg	1936	1503	405	20.9	Yes

[a] VAF: Variant allele frequen

[b] plasma DNA was evaluated by digital PCR

[c] This variant was evaluated by digital PCR, although the total allele was <200

[d] These variants were evaluated by digital PCR, although VAF was <10%

Supplementary Table S4. Treatment and outcomes of ESCC patients

Patient ID	First line therapy	Followed treatment with curative intent	Achieved to curative status	Relapse	Relapse site	Outcome
EC_1	surgery		yes	yes	lung	alive with cancer
EC_2	DCF	surgery	yes	no		alive
EC_3	DCF		no			cancer death
EC_4	DCF	CRT	no			cancer death
EC_5	surgery		yes	no		alive
EC_6	CF	surgery	yes	no	lymph node	alive
EC_7	DCF	CRT	yes	no		alive
EC_8	DCF		no			cancer death
EC_9	DCF		no			cancer death
EC_10	DCF		no			cancer death
EC_11	DCF		no			cancer death
EC_12	surgery		yes	no		alive
EC_13	DCF	CRT	yes	no	lymph node	alive
EC_14	DCF		no			cancer death
EC_15	DCF		no			cancer death
EC_16	DCF	surgery/CRT	yes	yes	liver	cancer death
EC_17	surgery		yes	no		alive
EC_18	DCF	CRT	yes	no		alive
EC_19	DCF		no			cancer death
EC_20	DCF	surgery	yes	no		alive
EC_21	DCF	surgery	yes	no		alive
EC_22	DCF	surgery	yes	no		alive
EC_23	surgery		yes	no		alive
EC_24	DCF	CRT	No			cancer death
EC_25	DCF	surgery	yes	no		non-cancer death
EC_26	DCF	CRT	no			cancer death
EC_27	surgery		yes	no		alive
EC_28	surgery		yes	no		alive
EC_29	DCF		no			alive with cancer
EC_30	CF	surgery	yes	yes	lymph node	alive
EC_31	surgery		yes	no		alive
EC_32	DCF	surgery	yes	no		alive
EC_33	DCF	CRT	no			cancer death
EC_34	surgery		yes	no		alive
EC_35	DCF	CRT	no			cancer death
EC_36	CF	surgery	yes	no		alive

Ce, Cervical esophagus ; Ut, upper thoracic esophagus; Mt, middle thoracic esophagus; Lt, Lower thoracic esophagus; DCF, Docetaxel/Cisplatin/5-FU; CF, Cisplatin/5-FU; CRT, chemoradiotherapy

Supplementary Table S5. Univariate analysis of overall survival for 34 ESCC patients

Factors	HR	95%CI	*P* value[a]
Pretreatment status			
Age (≥70/<70)	0.89	0.32-2.38	0.81
Gender (Female/Male)	0.86	0.20-2.66	0.81
Locus (Upper and middle/Lower)	0.63	0.20-1.74	0.38
Tumor depth (T1-3/T4)	0.19	0.06-0.52	0.0013*
Node involvement (N0, N1/N2, N3)	0.27	0.10-0.73	0.0101*
Tumor volume (<20cm^3/≥20cm^3)	0.15	0.0.-0.47	0.0007*
Number of mutation (≥5/≤4)	0.76	0.26-2.04	0.59
Pretreatment ctDNA (Negative/Positive)	0.46	0.11-1.43	0.19
NFE2L2 status (Wild type/Mutant)	0.69	0.25-2.19	0.50
ctDNA dynamics[b]			
ctDNA decrease at landmark (Yes/No)[a]	0.08	0.01-0.32	0.0001*

[a]P values are derived from Kaplan-Meier log-rank test

[b]analysis of 21 patients with positive pre-treatment ctDNA levels

Supplementary Table S6. dPCR-evaluated mutations duplicatedly detected in r

gene	Base change	Amino ccid change	Cases			
TP53	c.578A>G	p.His193Arg	EC_2	EC_30		
	c.578A>T*	p.His193Leu	EC_16			
	c.614A>G	p.Tyr205Cys	EC_2	EC_8	EC_18	EC_33
	c.659A>G	p.Tyr220Cys	EC_4	EC_6	EC_21	EC_36
	c.730G>A	p.Gly244Ser	EC_17	EC_28		
	c.844C>T	p.Arg282Trp	EC_26	EC_30		
NFE2L2	c.246A>T	p.Glu82Asp	EC_3	EC_4	EC_19	

dPCR, digital PCR

*different base change at the same genome position; Forward, reverse primers, and probe for wild type alleles were shared for dPCR analyses

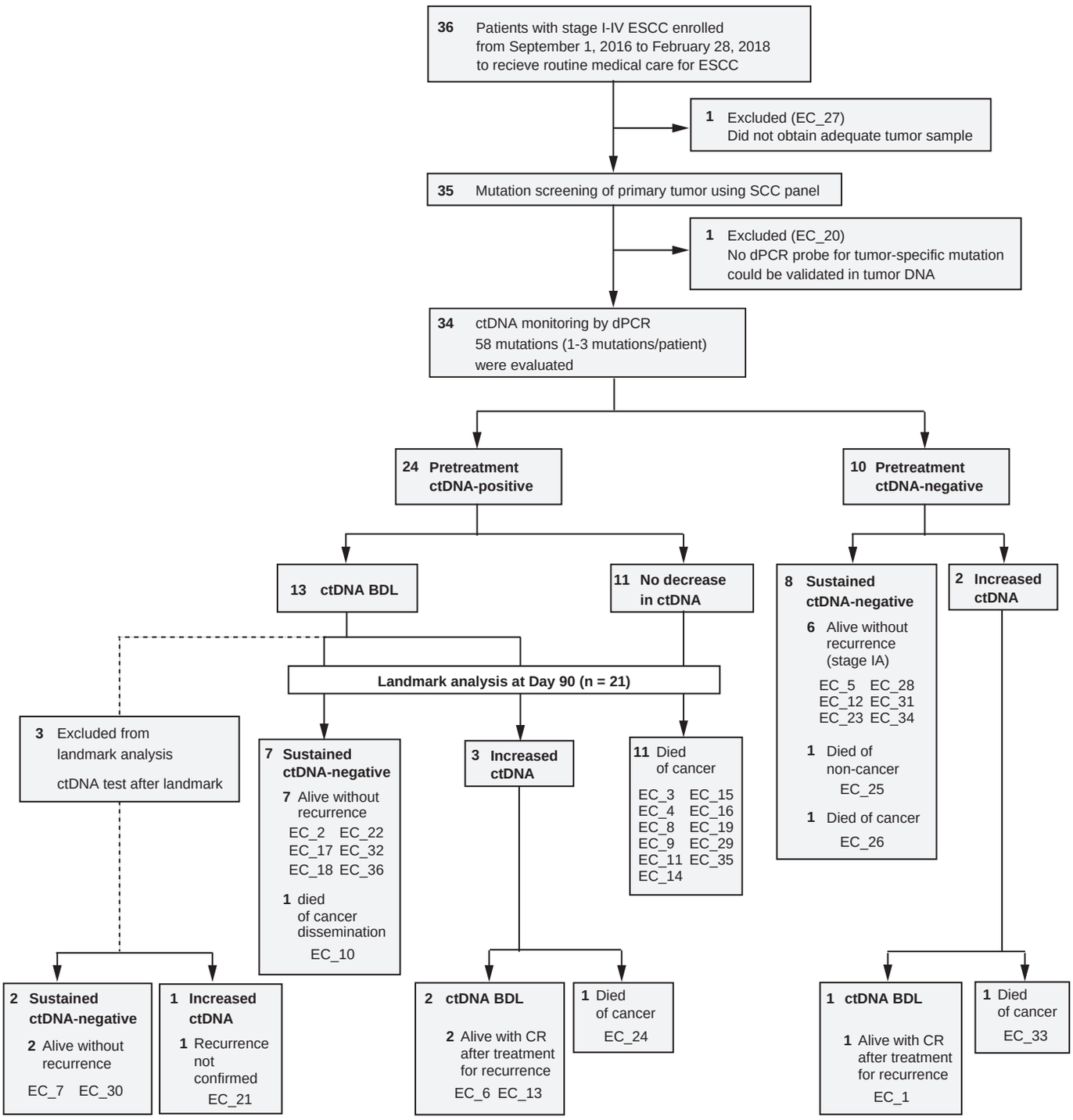

Supplementary Figure S1. Flow chart of patient outcomes

BDL, below detection limit; ctDNA, circulating tumor DNA; dPCR, digital PCR; ESCC, esophageal squamous cell carcinoma; SCC panel, squamous cell cancer panel.

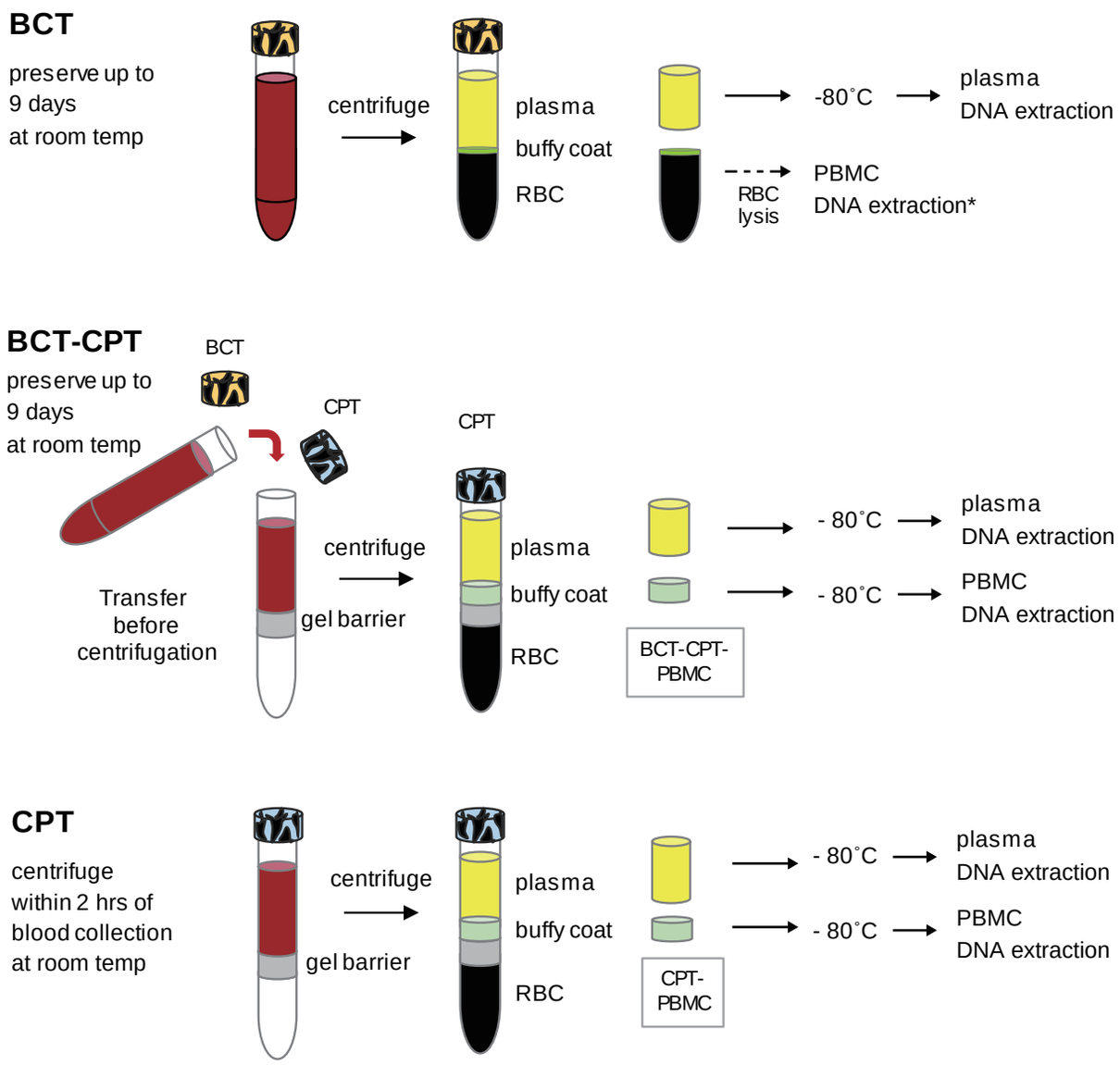

Supplementary Figure S2. Blood sample collection processes

Bottom: BCT tube. Top: CPT tube. Middle: combinatory tube method. CPT, Cell Preparation Tubes. BCT, Cell-Free DNA Blood Collection Tubes. RBC, red blood cell. PBMC, peripheral blood mononuclear cell. Asterisk, PBMC DNA can be extracted from remaining blood mixed with RBC and white blood cells using a Gentra Puregene Blood Kit (Qiagen, Hilden, Germany).

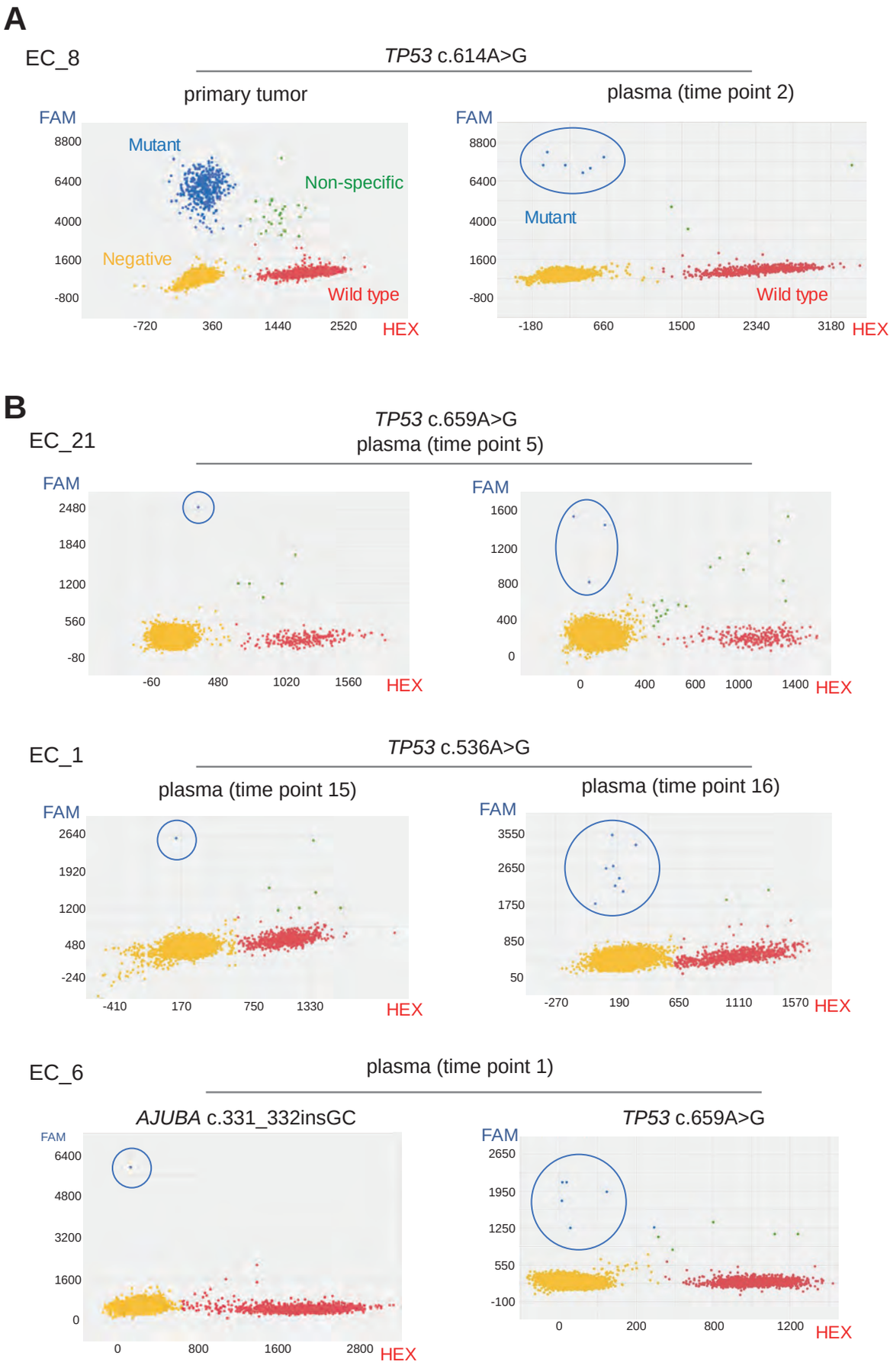

Supplementary Figure S3. ctDNA detection by digital PCR

(A) dPCR analysis in primary tumor and plasma samples. A specifically designed primer/probe set for the tumor-specific mutation *TP53* c.614A>G was validated using primary tumor DNA (left). After validation, ctDNA was counted in plasma DNA samples (right). (B) Criteria of positive-ctDNA determination. See eMethods 6. FAM, carboxyfluoscein.

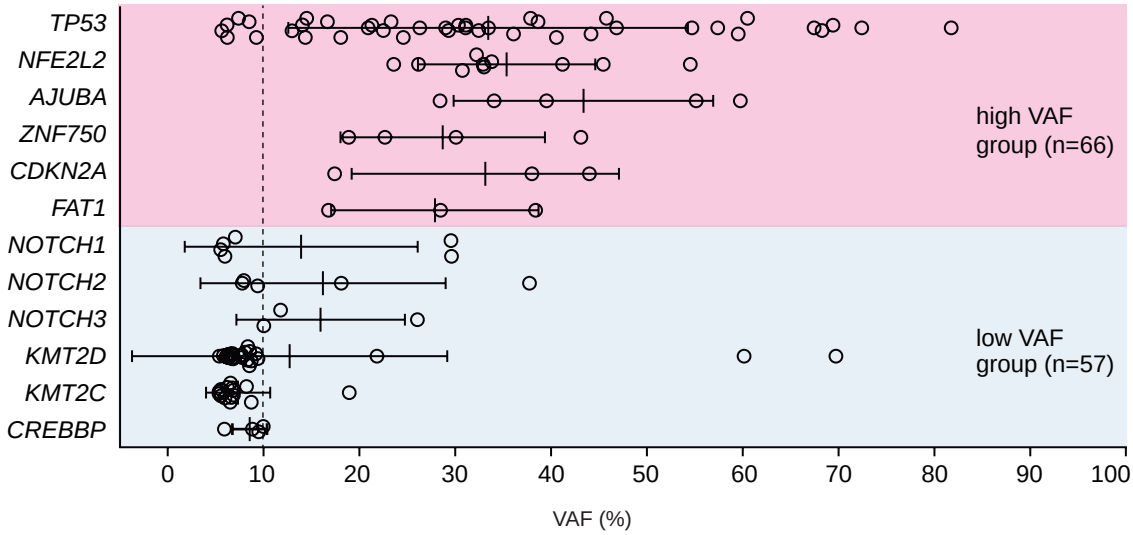

Supplementary Figure S4. Variant allele frequencies of mutated genes in primary tumors

VAF of genes that were mutated in 3 or more cases are shown. Average VAFs of 6 genes including *TP53*, *NFE2L2*, *AJUBA*, *ZNF750*, *CDKN2A*, and *FAT1* were >20% (33.9±35.7), while those for the remaining 6 genes including *NOTCH* family genes as well as *KMT2C*, *KMT2D*, and *CREBBP* were <20% (11.6±24.6).

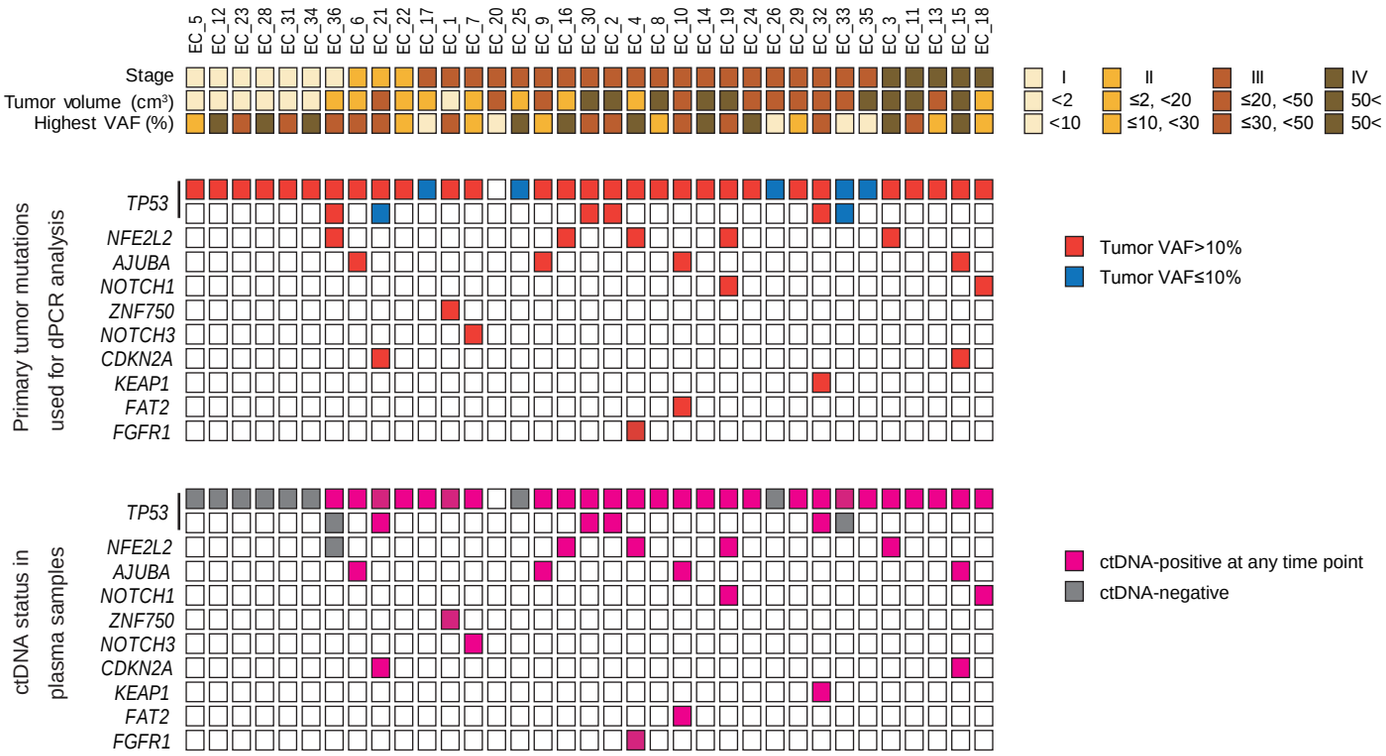

Supplementary Figure S5. Primary tumor-specific mutations and ctDNA in pretreatment plasma

TNM stage, tumor volume, and highest VAF of primary tumor mutation are shown in the top panel. Tumor-specific mutations validated by specifically-designed probes/primers for tumor DNA are colored in the middle panel. Red boxes, primary tumor VAF ≥10% by NGS analysis; blue boxes, primary tumor VAF <10% by NGS analysis. ctDNA status by dPCR of each mutation is shown in the bottom panel. Red boxes, ctDNA positive; gray boxes, ctDNA negative. ctDNA, circulating tumor DNA; dPCR, digital PCR; VAF, variant allele frequency.

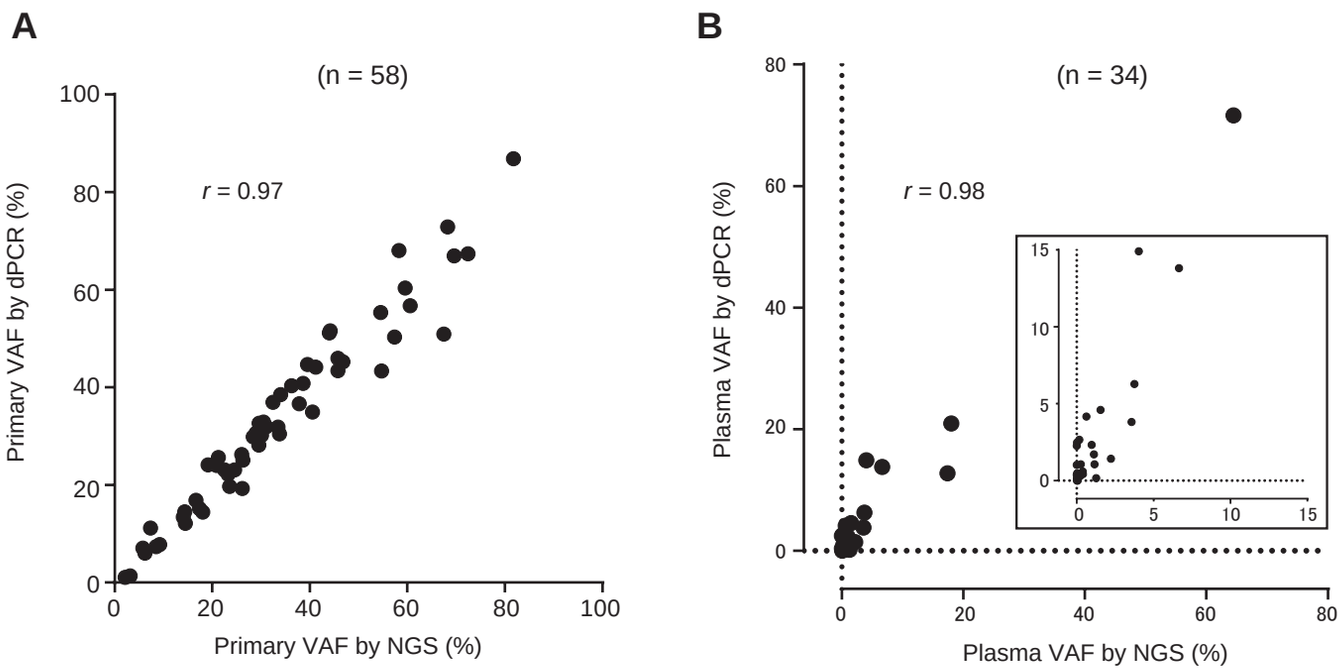

Supplementary Figure S6. Correlation between VAFs measured by NGS and dPCR

(A) Correlation between primary tumor VAFs measured by NGS and dPCR for 58 mutations (eTable 3; Spearman' s rank correlation coefficient). (B) Correlation between ctDNA VAFs of *TP53* mutations measured by NGS and dPCR (Spearman' s rank correlation coefficient). A total of 34 *TP53* mutations were detected in 28 patients having Stage IB or higher disease were evaluated. ctDNA, circulating tumor DNA; dPCR, digital PCR; NGS, next generation sequencing; VAF, variant allele frequency.

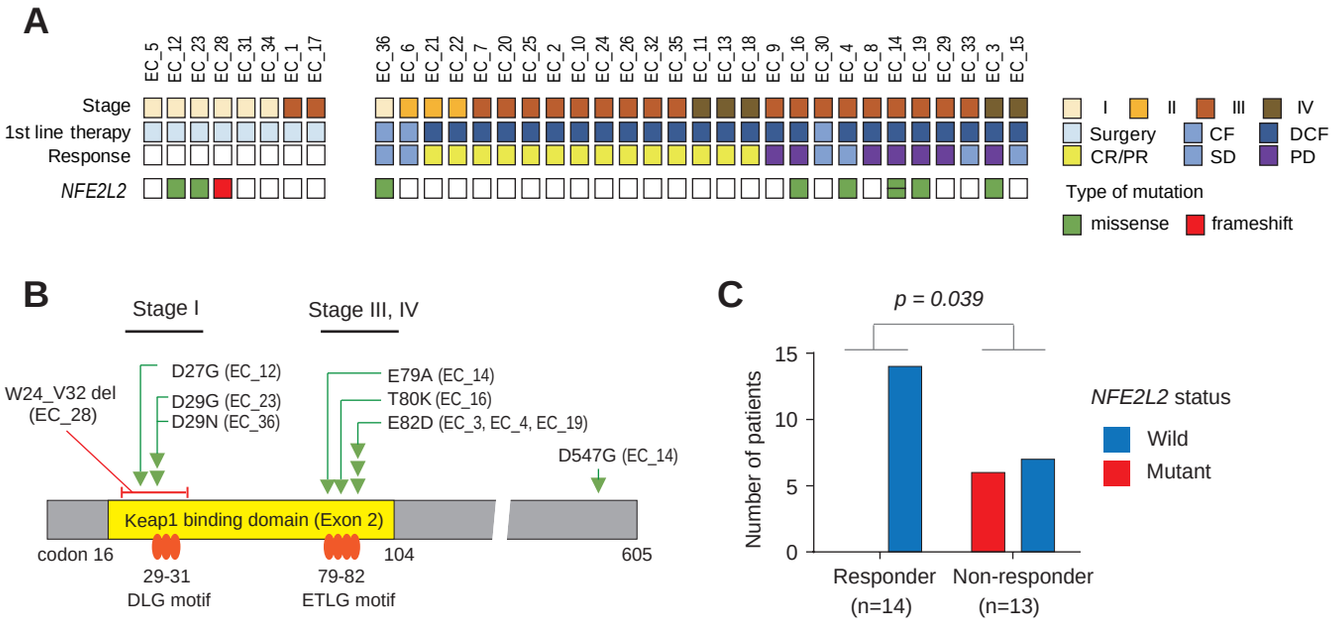

Supplementary Figure S7. *NFE2L2* mutations in primary tumors and chemotherapeutic response

(A) *NFE2L2* mutations and treatments for ESCC patients. First line therapies, response, and *NFE2L2* mutation are shown. (B) Mutation positions in the *NFE2L2* gene. The genetic position of *NFE2L2* mutations detected in primary tumors. CF, cisplatin/5-FU; CR, complete response; DCF, docetaxel/cisplatin/5-FU; dPCR, digital PCR; PD, progressive disease; PR, partial response; SD, stable disease. (C) Number of patients with *NFE2L2* status among chemotherapy responders and non-responders. Comparisons between Responders and Non-responders were performed by χ square test.

Supplementary Figure S8. Case presentations

Abbreviations in the case descriptions

BDL, below detection limit; CEA; carcinoembryonic antigen; CF, cisplatin/5-FU;
CIS, carcinoma in situ; CR, complete response; CYFRA 21-1, cytokeratin 19 fragments; DCF, docetaxel/cisplatin 5-FU; CRT, chemoradiotherapy; LN, lymph node;
PD, progressive disease; PT, proton beam therapy; PTX, paclitaxel; PR, partial response; RT, radiotherapy; SCC, squamous cell carcinoma antigen; SD, stable disease;

EC_1 Stage IIIA

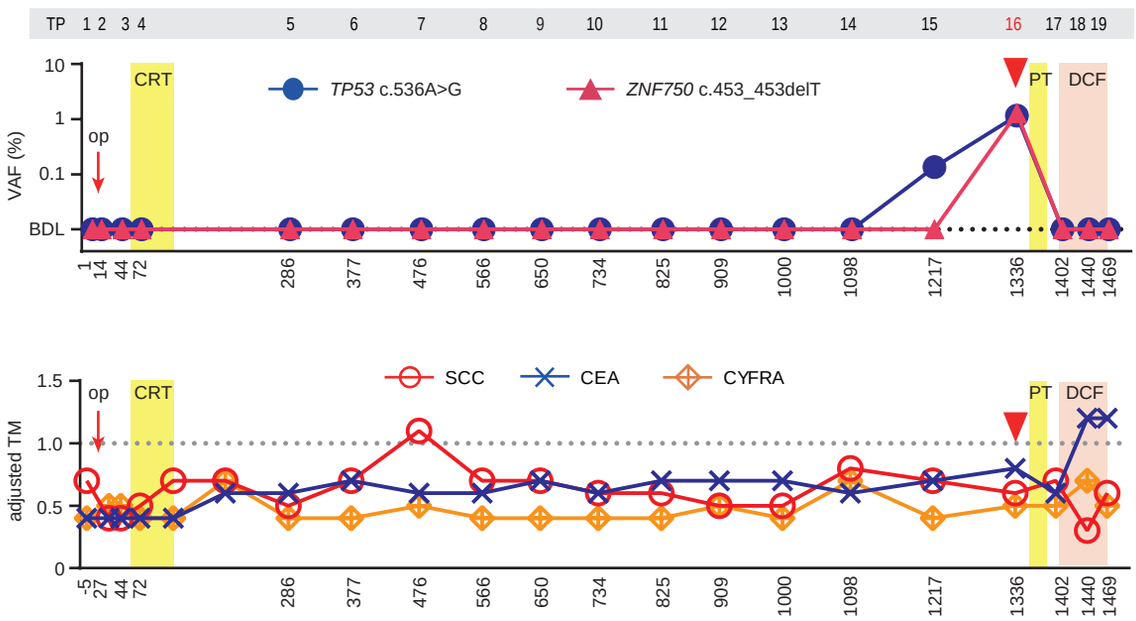

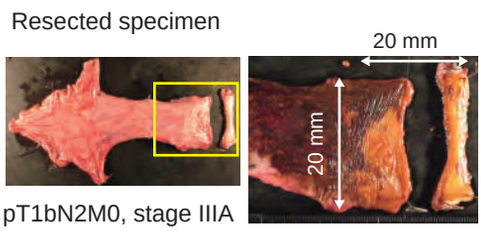

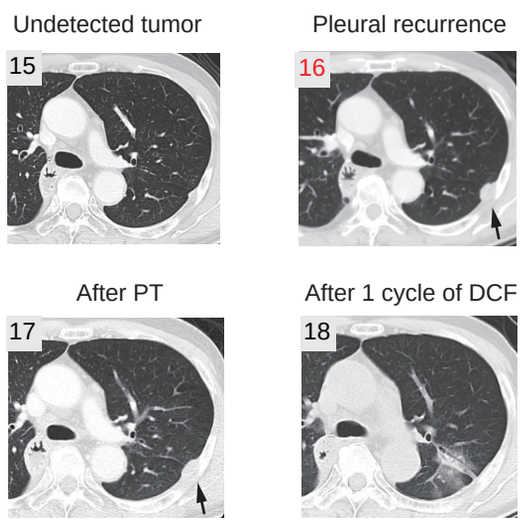

EC_1 had a superficial ESCC in the upper third of the esophagus and metastasis could not be detected in a pre-treatment CT scan. Surgical resection was undertaken as first line therapy. Whole and enlarged images of the resected specimen are presented. Microscopically, primary tumor with submucosal invasion and three mediastinal lymph node metastases were observed. Resected margin of the primary tumor on the oral side of the esophagus was not sufficient and adjuvant CRT was followed. In addition, ctDNAs of *TP53* c.536A>G and *ZNF750* c.453_453delT were not detected in plasma DNA from pretreatment to TP 14. A left pleural nodule was evident at day 1,336 (TP16, arrow), but neither CT scan nor tumor marker could determine whether this tumor was secondary primary lung cancer, ESCC recurrence, or other non-specific findings. However, as ctDNAs for both mutations were detected at TP16, the tumor could be diagnosed as ESCC recurrence. In addition, ctDNA of *TP53* c.536A>G was already elevated 4 months before tumor detection by CT scan (TP15). After proton beam therapy, the tumor was reduced and ctDNA decreased to zero at day 1,402 (TP 17). The tumor became undetectable after 1 additional cycle of DCF (TP 18). Red arrowheads in the upper panels indicate the time point at which recurrence was clinically evident.

EC_2 Stage IIIC

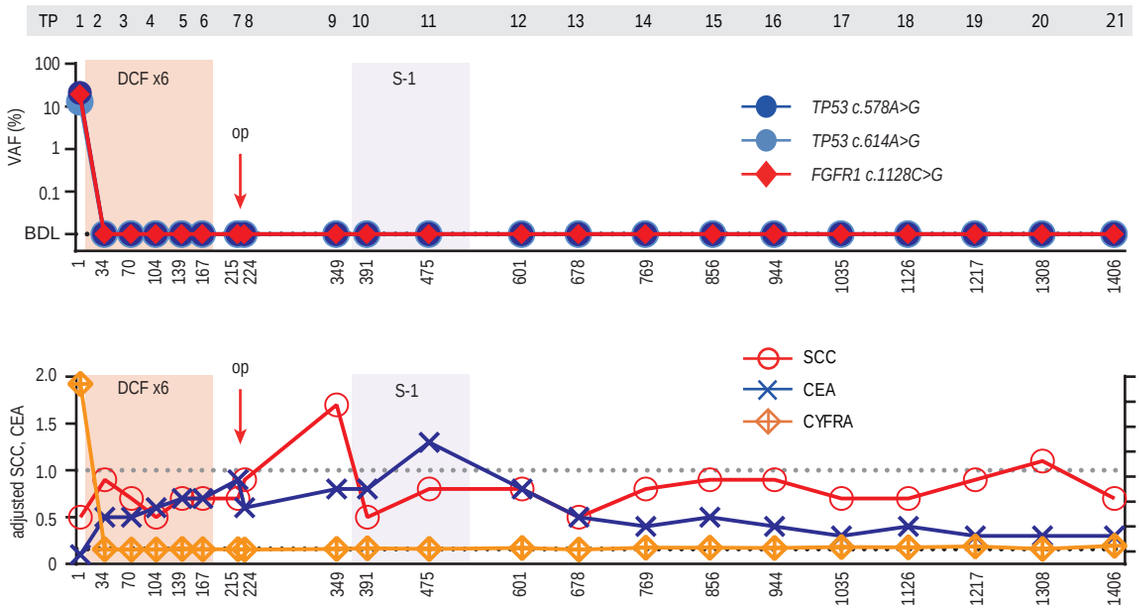

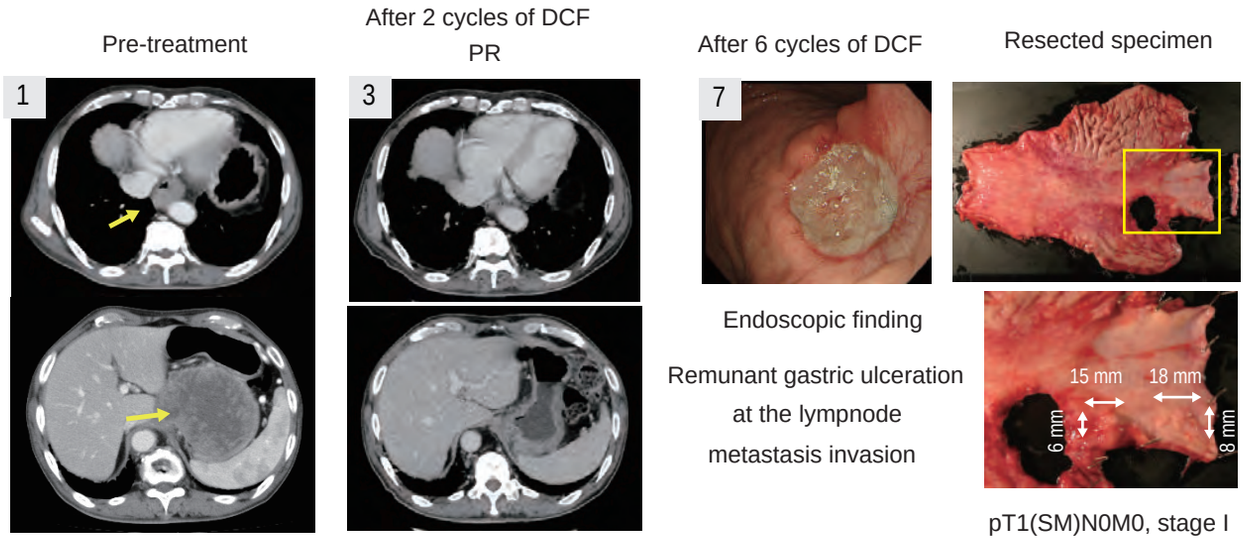

EC_2 had a primary ESCC with adventitia invasion in the lower third of the esophagus and significant abdominal lymph node metastasis that had invaded the stomach (TP 1, arrows). Marked tumor shrinkage was achieved after 2 cycles of DCF (TP 3). After 6 cycles of DCF, a remnant of the primary ESCC tumor and a deep gastric ulcer were endoscopically observed in the stomach wall where the abdominal lymph node metastasis had invaded before administration of chemotherapy (TP 7). In the resected specimen, remnant tumor cells were limited to the submucosal layer in areas of the gastroesophageal junction (15 x 6 mm^2) and the lower esophagus (18 x 8 mm^2) (TP 7). Patient-specific ctDNAs were monitored using three patient-specific mutations in *TP53* c.578A>G, *TP53* c.614A>G, and *FGFR1* c.1128C>G. After one cycle of DCF, levels of all ctDNAs were decreased below the detection limit and were sustained as ctDNA-negative until TP 21 with no recurrence.

EC_3 Stage IV

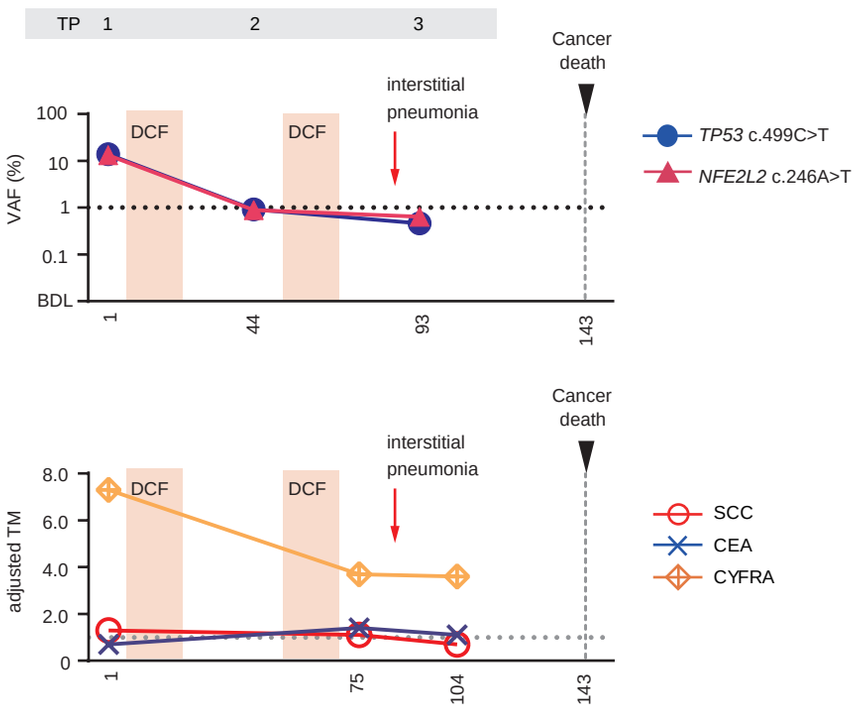

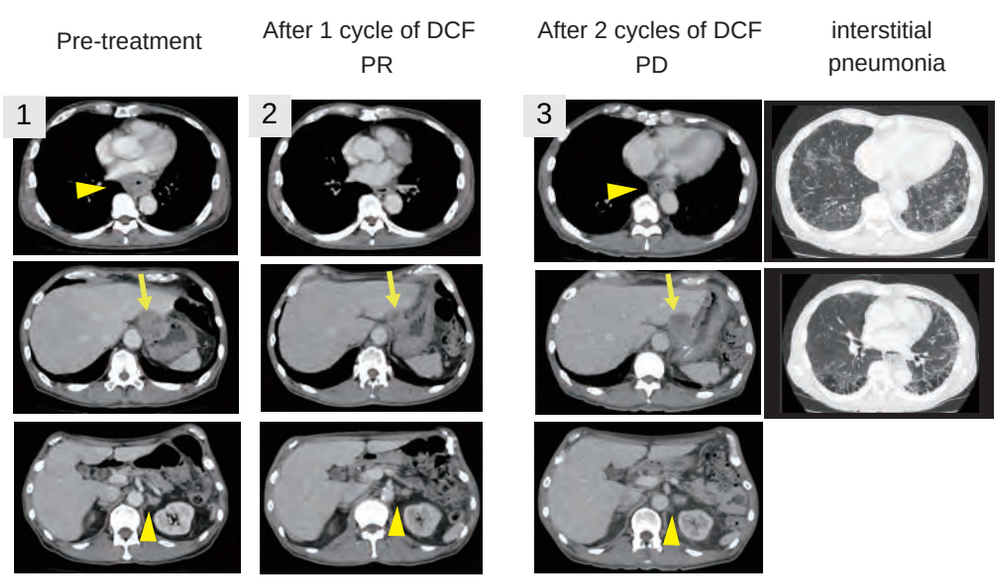

EC_3 had a primary ESCC with adventitia invasion in the middle third of the esophagus (horizontal arrowhead), multiple abdominal lymph node metastases (arrows), and hematogenous metastasis in the left adrenal gland (vertical arrowhead) (TP 1-3). Although the tumor size was temporarily reduced after the first cycle of DCF, the patient had tumor regrowth and interstitial pneumonia by the end of the second cycle of DCF. The patient died of cancer progression on Day 143. In pre-treatment plasma, the ctDNA levels of *TP53* c.499C>T and *NFE2L2* c.246A>T were 13.80% and 13.27%, respectively. Levels of ctDNA for both mutations decreased to <1% after chemotherapy but remained detectable.

EC_4 Stage IIIC

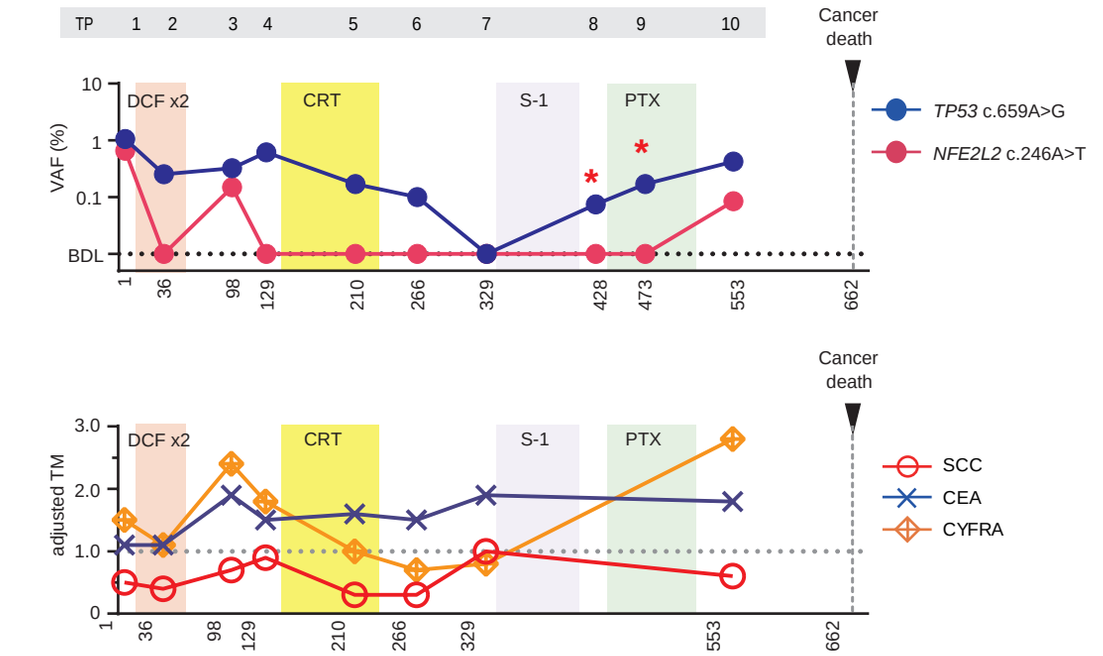

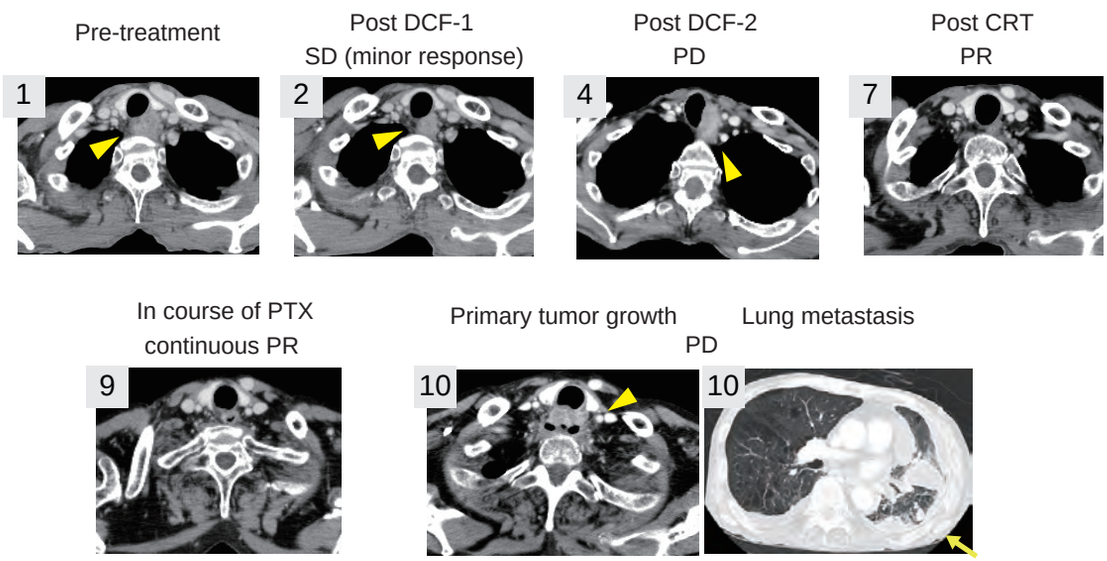

EC_4 had cervical ESCC that invaded to the trachea (TP 1). Minor response was observed after the first cycle of DCF chemotherapy (TP 2); the tumor showed regrowth after the second cycle of DCF (TP 4). Remarkable shrinkage of the tumor was observed after CRT (TP 7). The level of *TP53* c.659A>G ctDNA was temporarily decreased below the detection limit after CRT. Due to adverse effects including diarrhea and dehydration, S-1 chemotherapy was changed to weekly paclitaxel therapy. Primary tumor regrowth and lung metastasis were detected by CT (TP 10). The patient died of cancer on Day 662. Arrowheads and arrow indicate primary tumor and lung metastasis, respectively. Asterisks indicate early elevation of ctDNA before tumor regrowth was confirmed by CT.

EC_5 Stage IA

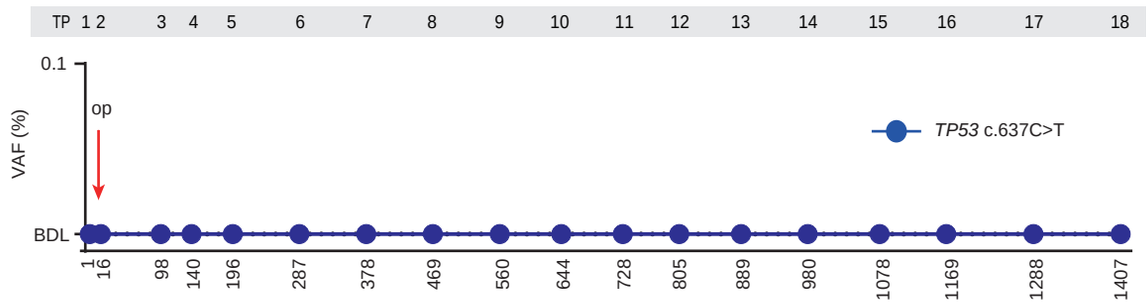

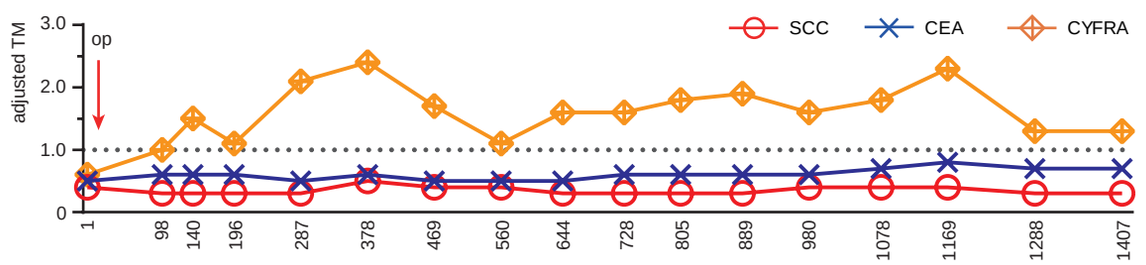

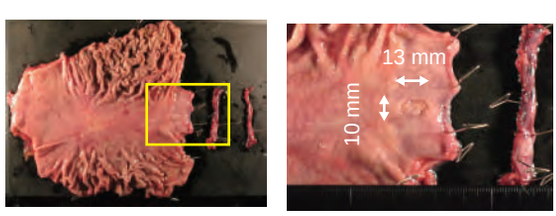

Resected specimen

pT1bN0M0, stage IA

EC_5 had surgical resection for superficial ESCC in the abdominal esophagus. The tumor was 13 x 10 mm^2 and microscopically the invasion was limited to the submucosal layer. No lymph node metastasis was observed.

EC_6 Stage IIA

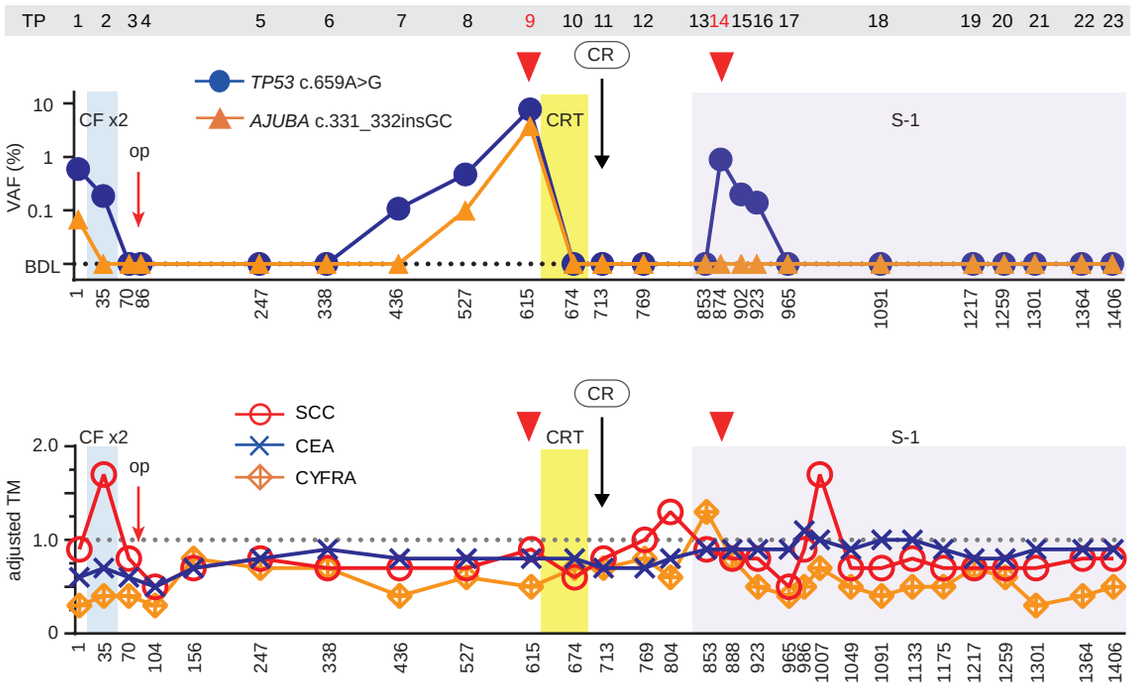

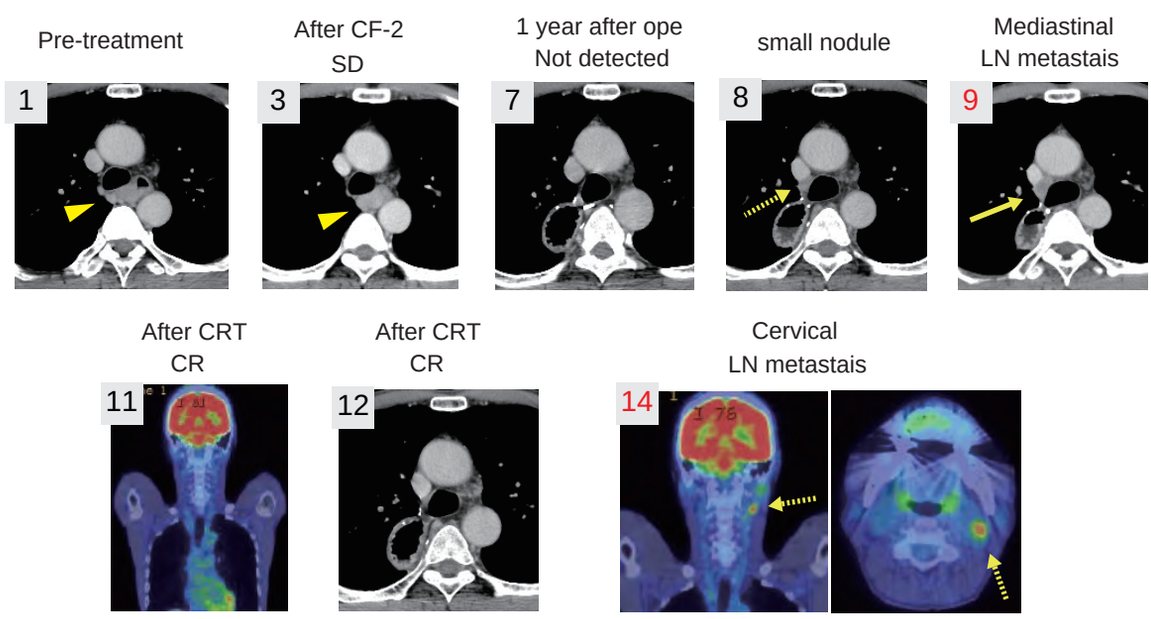

EC_6 had a primary ESCC with adventitia invasion in the upper third of the esophagus and no lymph node metastasis (TP 1). This case was diagnosed T3N0M0, Stage IIA. Two cycles of neoadjuvant CF followed by surgical resection were completed. Adventitia invasion by the primary tumor and negative lymph node metastasis were also confirmed pathologically. At 18 months (545 days) after surgical resection, a 8 x 4 mm^2 mediastinal tracheal lymph node metastasis was detected by CT scan (TP 9). The patient achieved CR after CRT for the mediastinal lymph node (TP 11). The patient received an oral adjuvant therapy of S-1 for one year. Red arrowheads in the upper panels indicate the time point when recurrence is clinically evident. Yellow arrowheads and arrows in CT images indicate primary tumor and lymph node metastasis, respectively. Dashed arrows indicate lesions classified as non-specific findings at the time of diagnosis.

EC_7 Stage IIIA

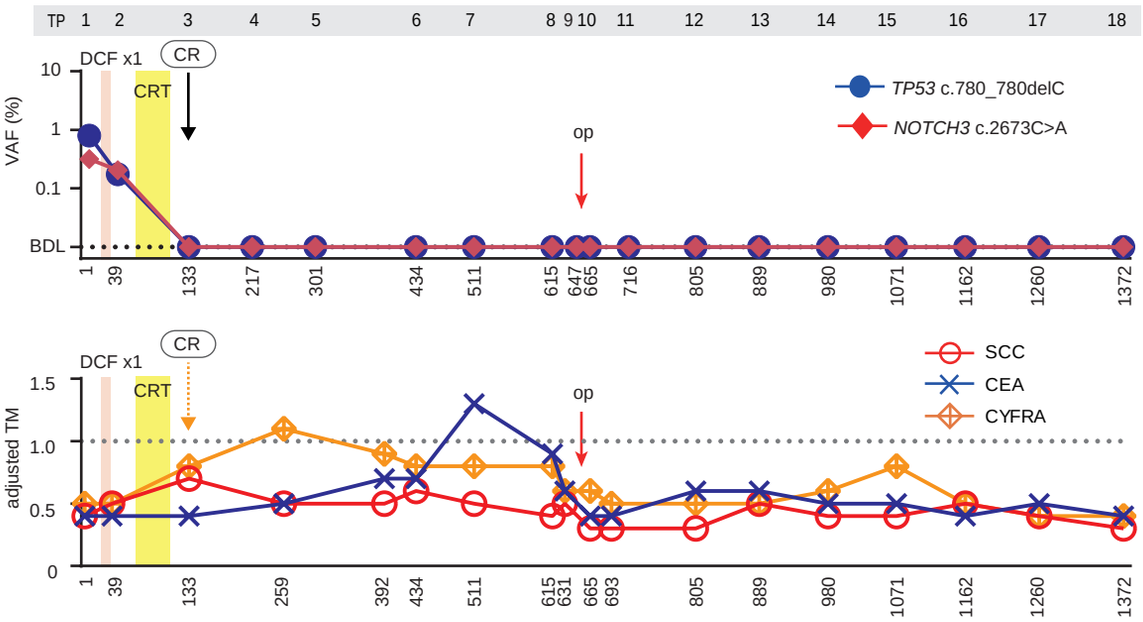

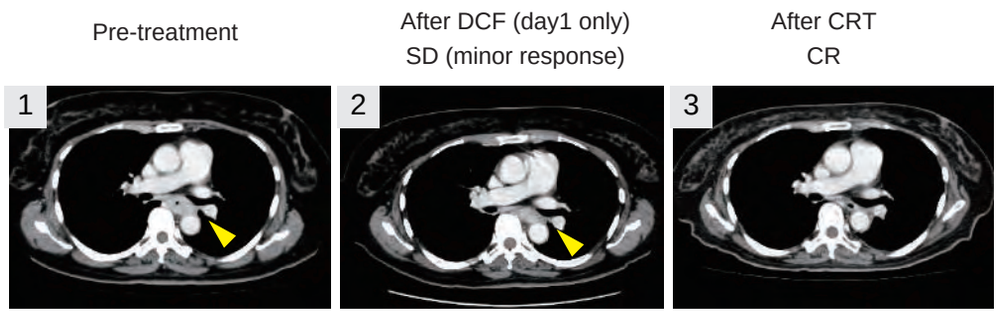

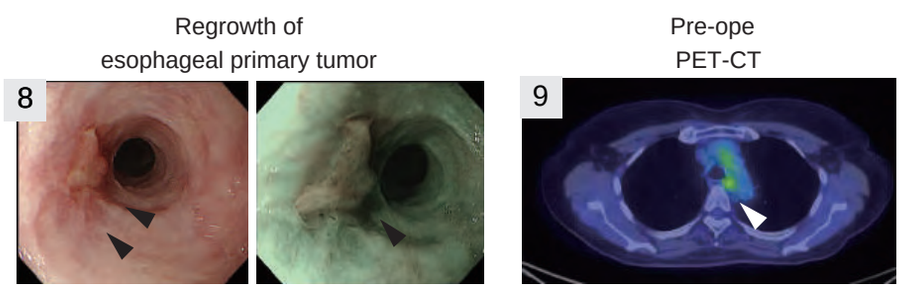

EC_7 had a primary ESCC with adventitia invasion in the middle and upper third of the esophagus with a mediastinal lymph node metastasis. This case was diagnosed as T3N1M0, Stage IIIA. Although chemotherapy with DCF was initiated, the treatment was aborted on Day 2 of the first cycle due to liver dysfunction. An alternative CRT with low-dose cisplatin and 5-FU achieved CR. After 1.5 yr, an esophageal tumor with a mild FDG accumulation was observed on PET-CT scan (TP 8 and 9). A salvage esophagectomy was performed and cancer cells were not observed in the resected specimen. Recurrence was not observed until Day 1,372. Yellow arrowheads in CT images indicate the primary tumor. Black arrowheads in endoscopic images and a white arrowhead in PET-CT image indicate a non-malignant esophageal tumor.

EC_8 Stage IIIC

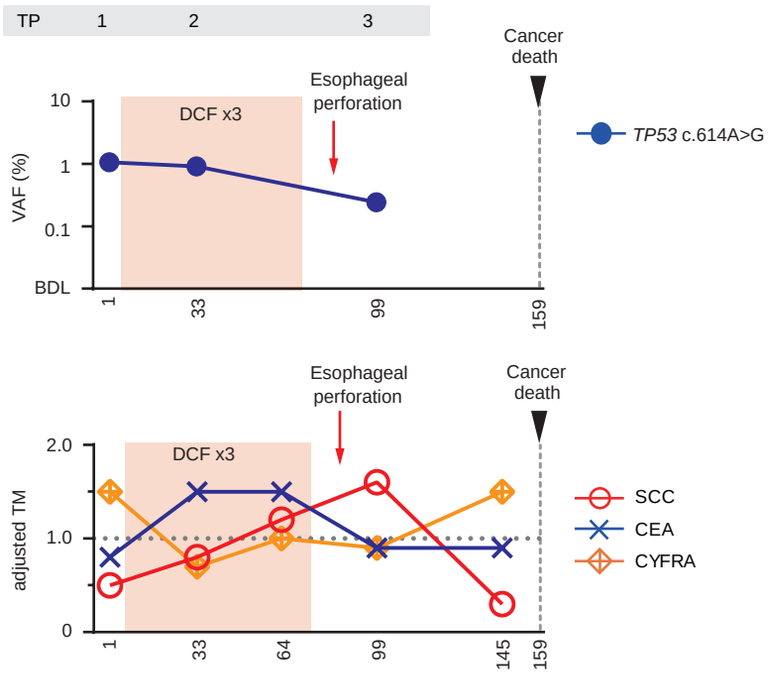

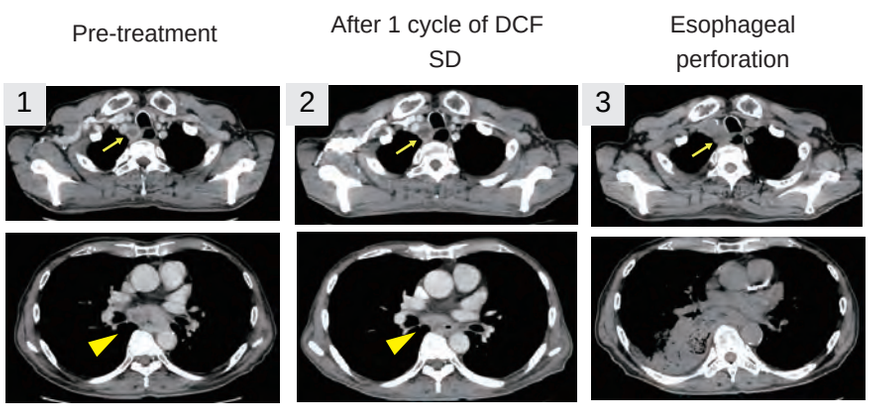

EC_8 had an ESCC in the middle, upper and lower third of the esophagus that had invaded the right lung and right subcranial recurrent nerve; metastasis to the main bronchus lymph nodes also occurred (TP 1). This case was diagnosed as T4bN2M0, Stage IIIC. After 3 cycles of DCF, penetration of the esophageal primary tumor into the right lung was observed (TP 3). The patient died of cancer progression on Day 159.

EC_9 Stage IIIB

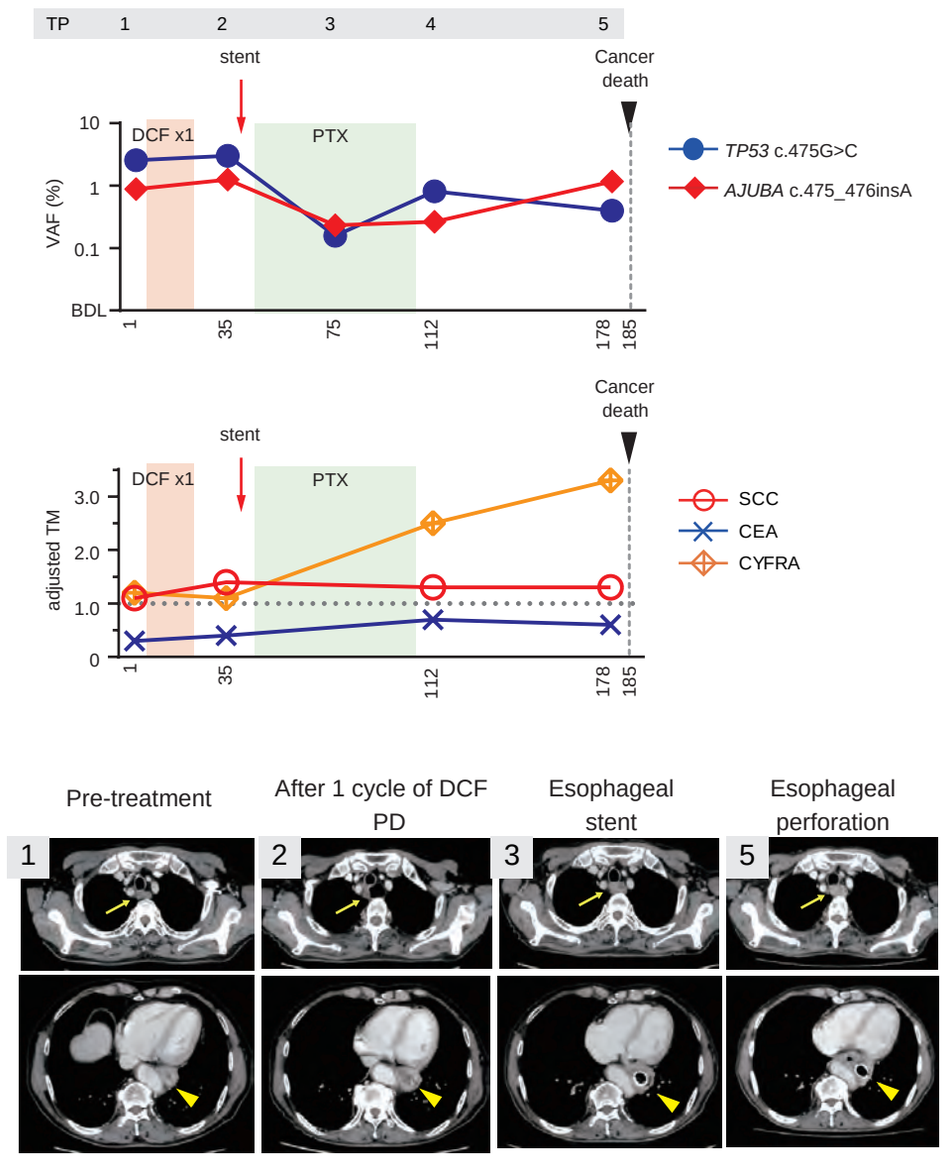

EC_9 had a primary ESCC with adventitia invasion in the middle and lower third of the esophagus. Metastatic sites including a bilateral recurrent nerve lymph node and lesser curvature lymph node of the stomach along with branches of the left gastric artery were observed. This case was diagnosed T3N2M0, Stage IIIB. Disease progression was observed after the first cycle of DCF, and an esophageal stent was then placed at the stricture of the primary tumor (TP 2 and 3). Although paclitaxel was given weekly for two months, the patient died of cancer progression on Day 185. Esophageal perforation was also observed by CT scan at TP 5. Arrowheads and arrows indicate primary tumor and lymph node metastasis, respectively.

EC_10 Stage IIIC

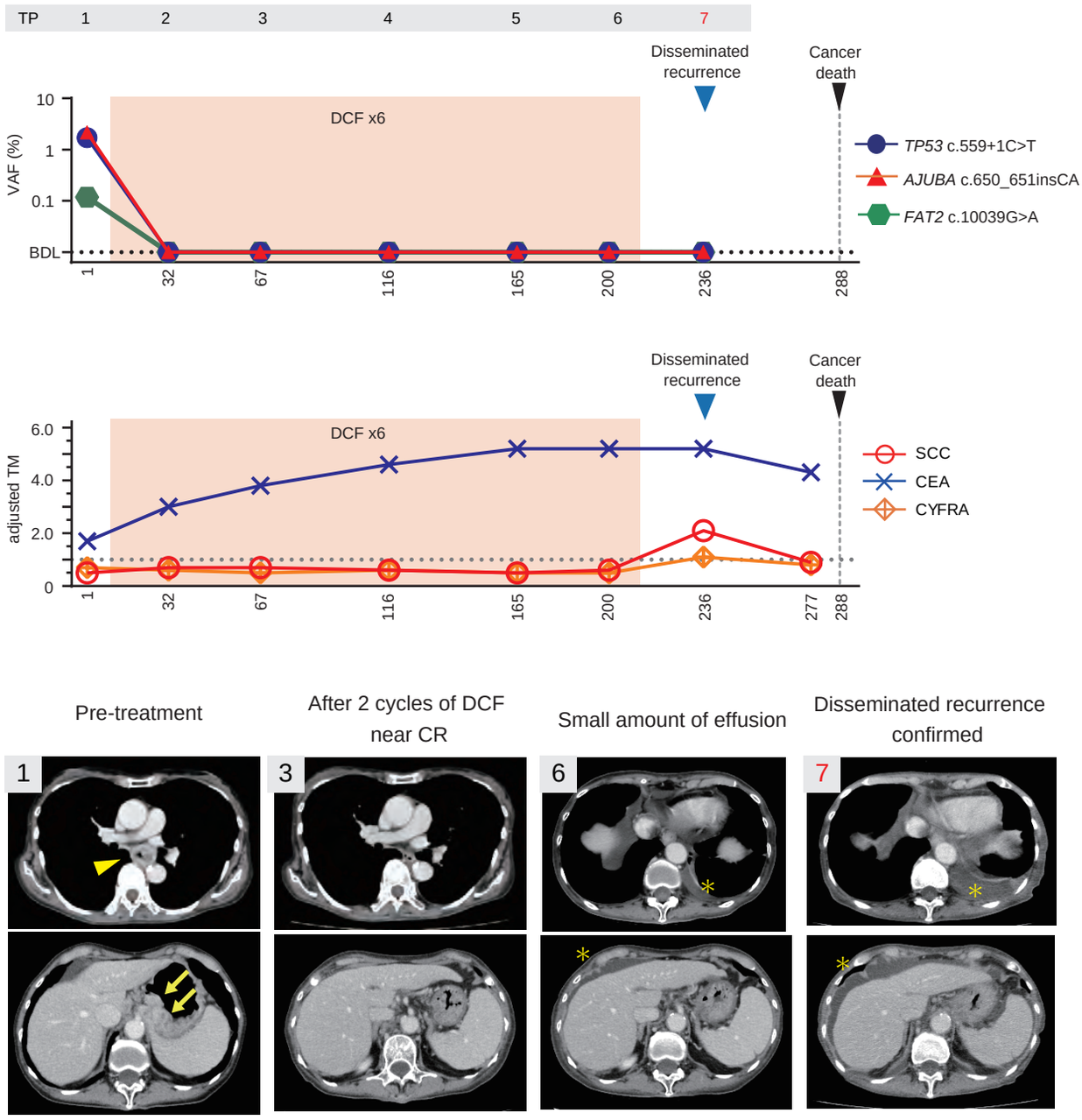

EC_10 had a primary ESCC with adventitia invasion in the lower third of the esophagus and abdominal lymph node metastasis that invaded to the stomach (TP 1). Remarkable tumor shrinkage was observed after the first 2 cycles of DCF, whereas ctDNA levels of all mutations were decreased below the detection limit after the first cycle of DCF (TP 2). However, after 5 cycles of DCF, a small amount of effusion was detected by CT scan (TP 6). Pleural effusion and ascites rapidly increased and the patient died of disseminated recurrence 2 months after diagnosis. Blue arrowheads in the upper panels indicate the time point when recurrence was clinically evident. The yellow arrowhead and arrows in CT images indicate primary tumor and lymph node metastases, respectively. Yellow asterisks indicate pleural effusion and ascites.

EC_11 Stage IV

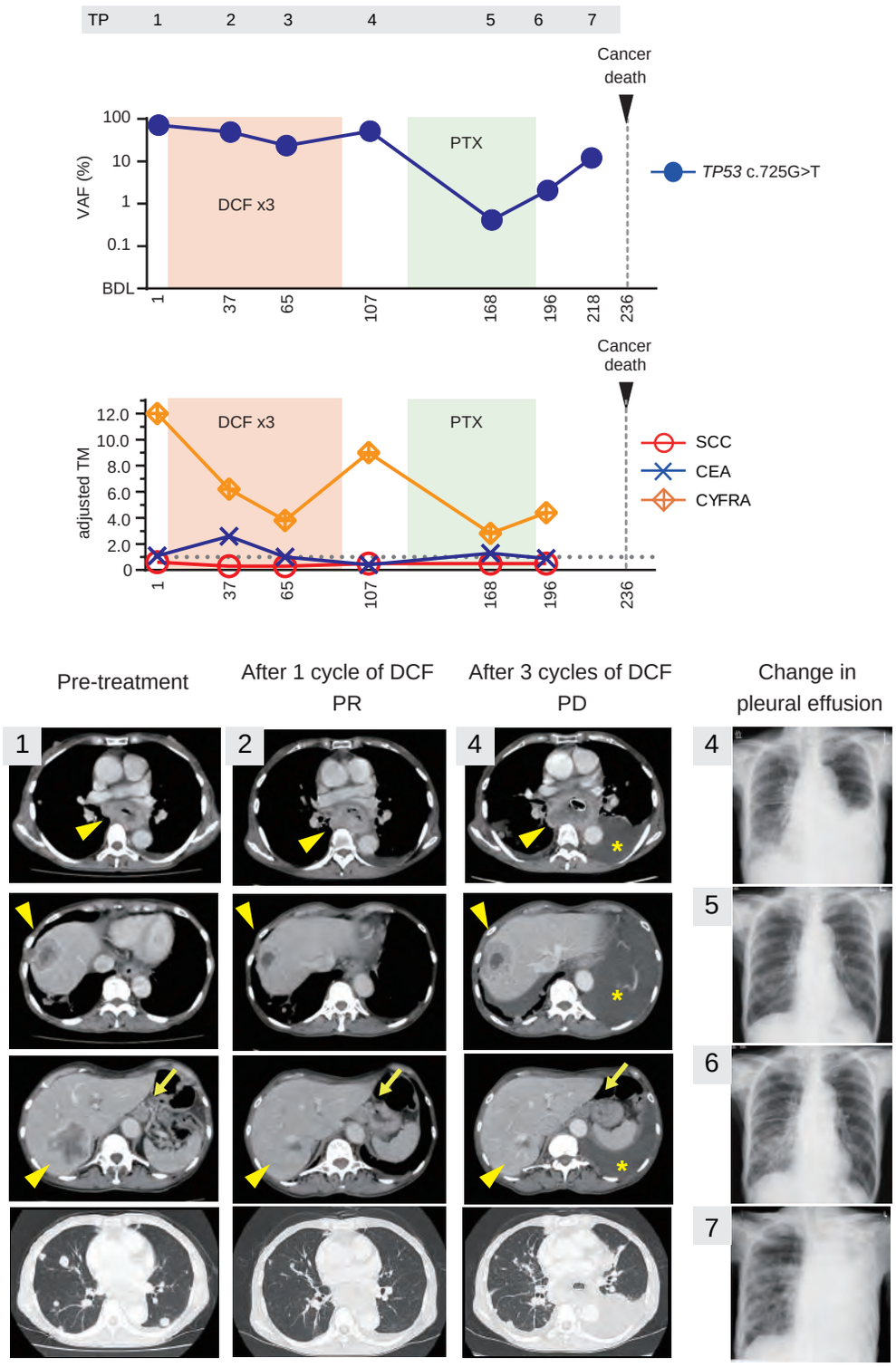

EC_11 had a primary ESCC with adventitia invasion in the middle, upper and lower third of the esophagus, multiple mediastinal and abdominal lymph node metastases, and multiple hematogenous metastasis in the liver and bilateral lungs (TP 1). This case was diagnosed T3N3M1, Stage IV. Although metastatic lesions were reduced by administration of DCF, primary tumor growth and left pleural effusion were evident after the third cycle of DCF (TP 4). Weekly paclitaxel therapy temporarily reduced the pleural effusion (TP 4-7), but the patient died of cancer progression on Day 236. Arrowheads in CT images indicate primary tumor and liver metastasis, whereas arrows indicate lymph node metastasis. Yellow asterisks indicate pleural effusion and ascites.

EC_12 Stage IA

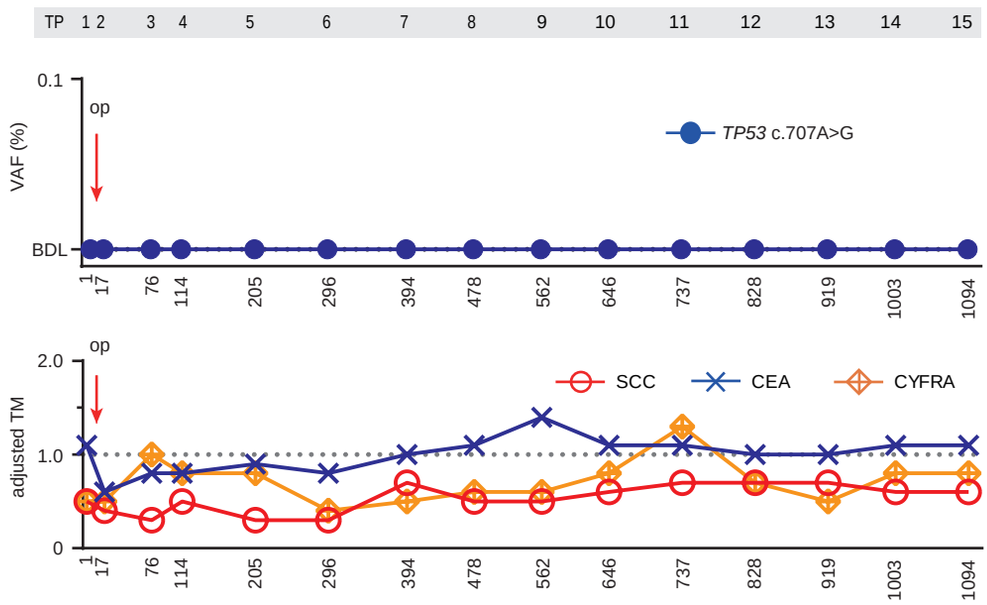

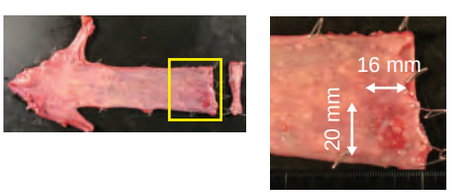

Resected specimen
pT1bN0M0, stage IA

EC_12 had superficial ESCC in the middle third of the esophagus that was surgically resected. The tumor was 16 x 20 mm^2 and microscopically confirmed tumor invasion was limited to the submucosal layer. No lymph node metastasis was observed.

EC_13 Stage IV

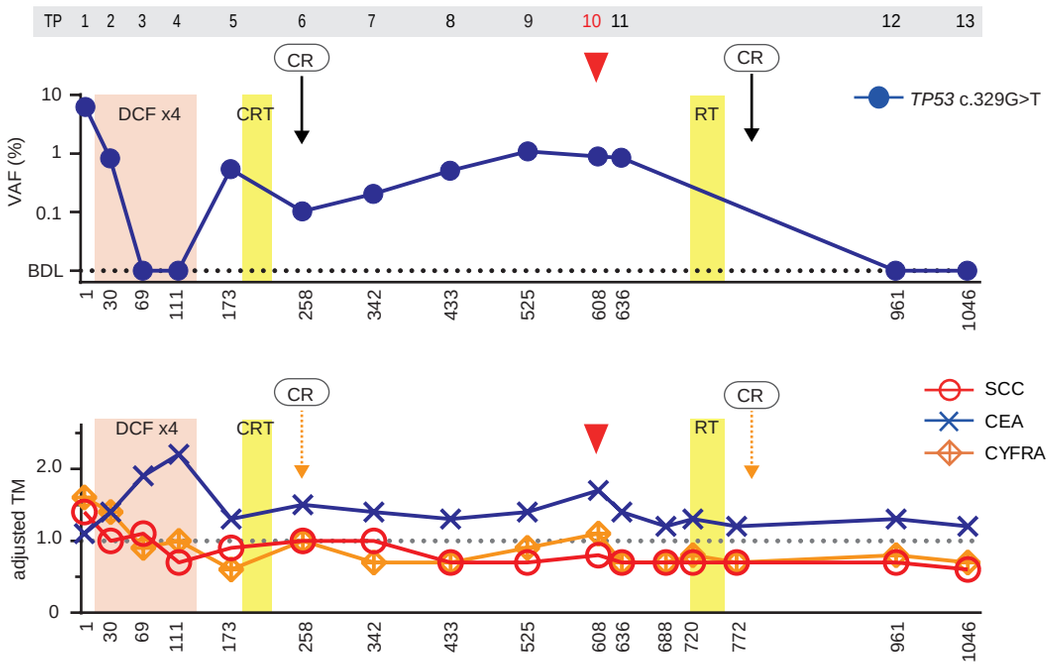

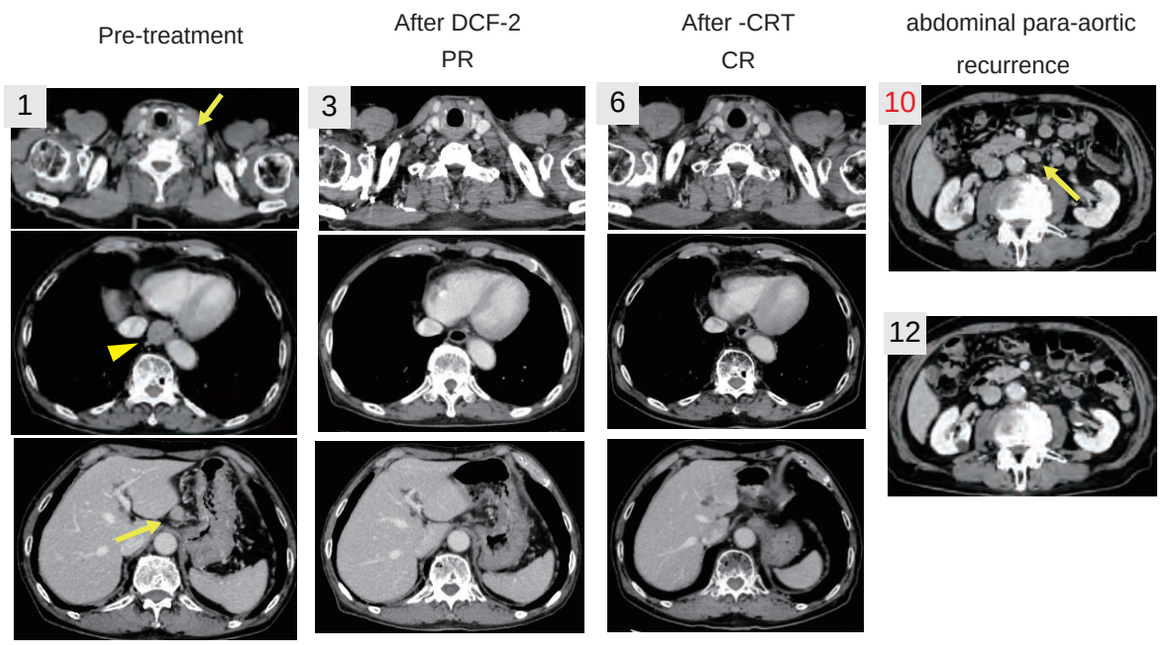

EC_13 had a primary ESCC with adventitia invasion in the lower third of the esophagus with multiple lymph nodes metastasis in mediastinal, abdominal, and cervical regions (TP 1). As the cervical metastatic node was extra-regional metastasis, this case was diagnosed T3N1M1, Stage IV. Four cycles of DCF followed by CRT achieved CR (TP 6). An abdominal para-aortic lymph node metastasis was observed by CT on Day 608 (TP 10). Red arrowheads in the upper panels indicate the time point when recurrence was clinically evident. A yellow arrowhead and arrows in CT images indicate primary tumor and lymph node metastasis, respectively.

EC_14 Stage IIIB

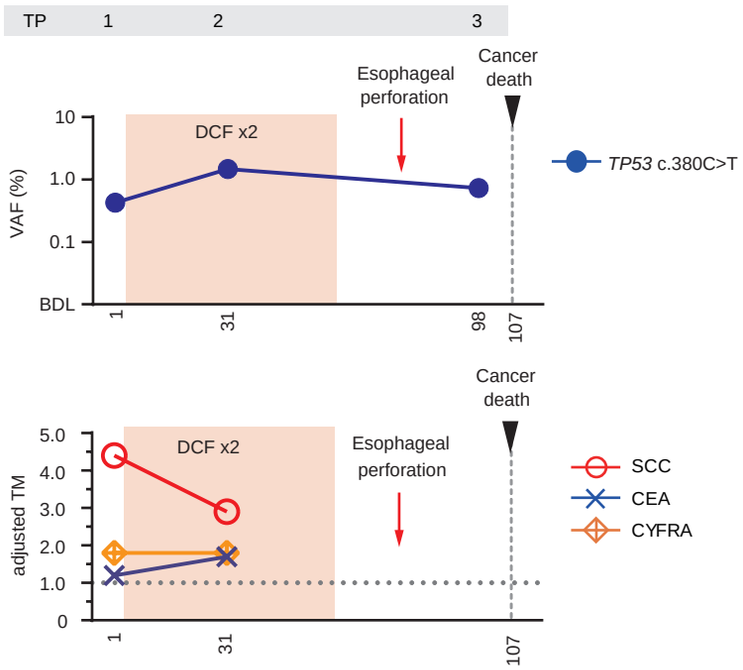

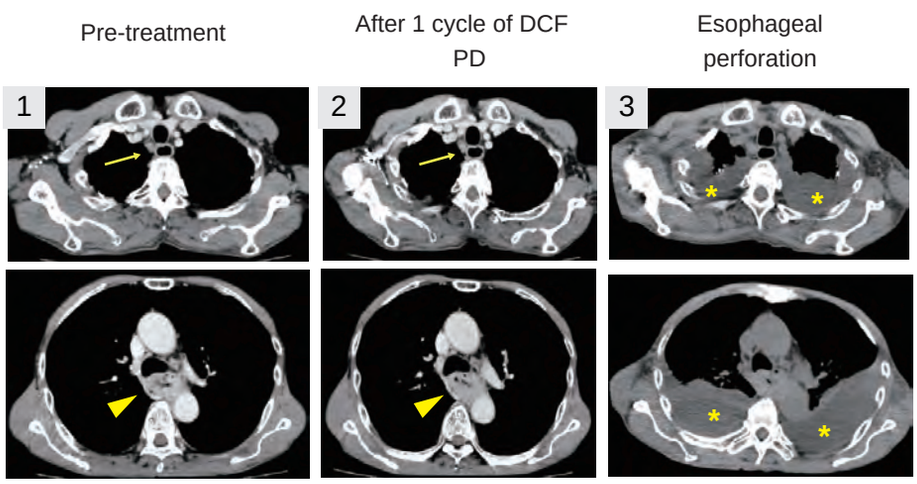

EC_14 had ESCC that invaded the trachea in the upper and middle third of the esophagus with multiple mediastinal lymph nodes metastasis. This case was diagnosed T4bN2M0, Stage IIIC. Disease progression and esophageal perforation were observed after the first and second cycle of DCF therapy (TP 2 and 3). The patient died of cancer progression on Day 107. Yellow arrowhead and arrows in CT images indicate primary tumor and lymph node metastasis, respectively. Yellow asterisks indicate pleural effusion.

EC_15 Stage IV

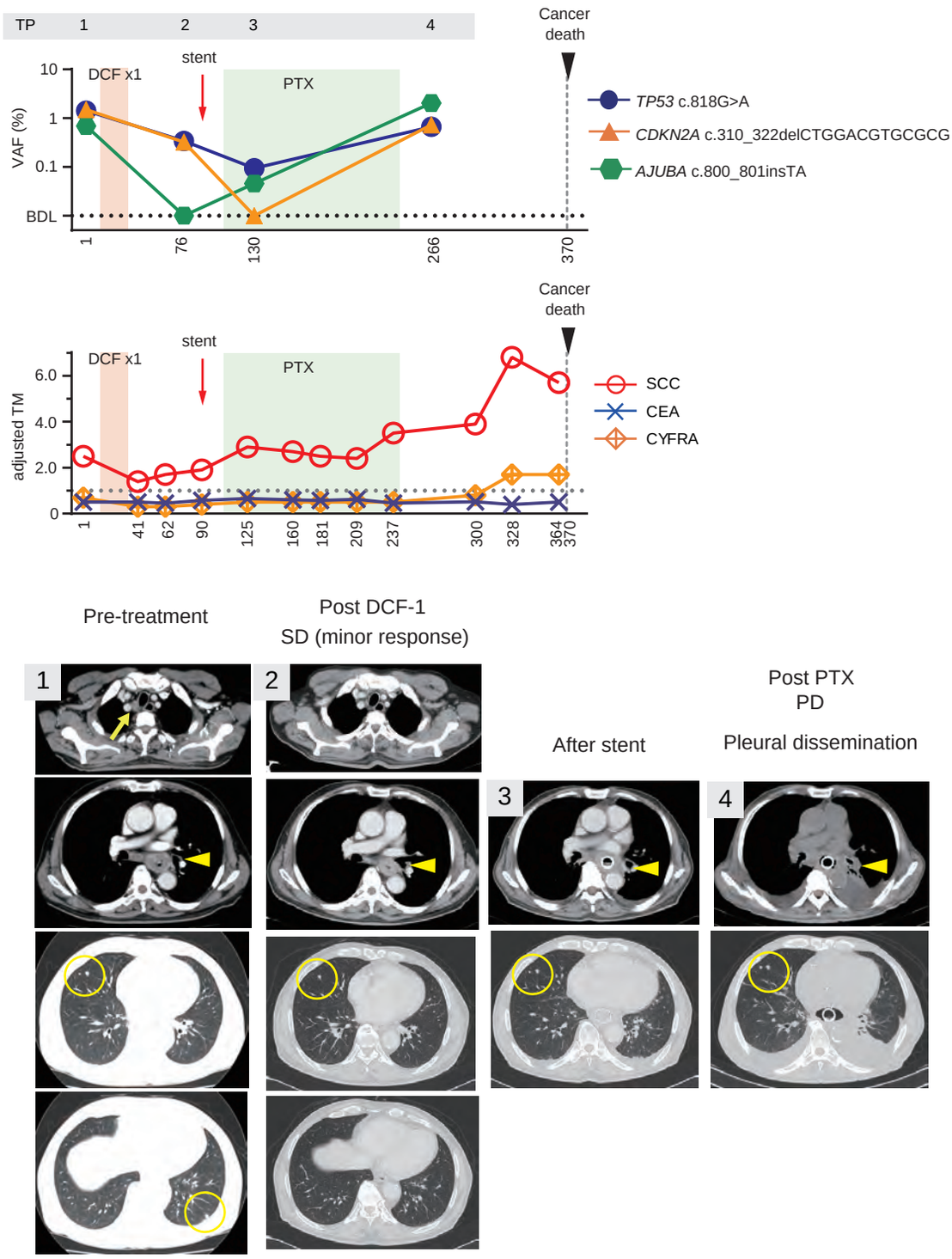

EC_15 had an ESCC in the middle and upper third of the esophagus, invasion of the left main bronchus, multiple mediastinal lymph node metastases, and bilateral hematogenous metastases in the lung (TP 1). This case was diagnosed T4bN2M1, Stage IV. After the first cycle of DCF, shrinkage of mediastinal lymph node metastases was observed, although esophageal stenosis persisted (TP 2). An esophageal stent was placed followed by weekly paclitaxel for 6 months. With subsequent primary tumor growth and pleural dissemination, the patient died of cancer progression on Day 370. Yellow arrowheads and an arrow in CT images indicate primary tumor and lymph node metastasis, respectively. Yellow circles indicate lung metastases.

EC_16 Stage IIIB

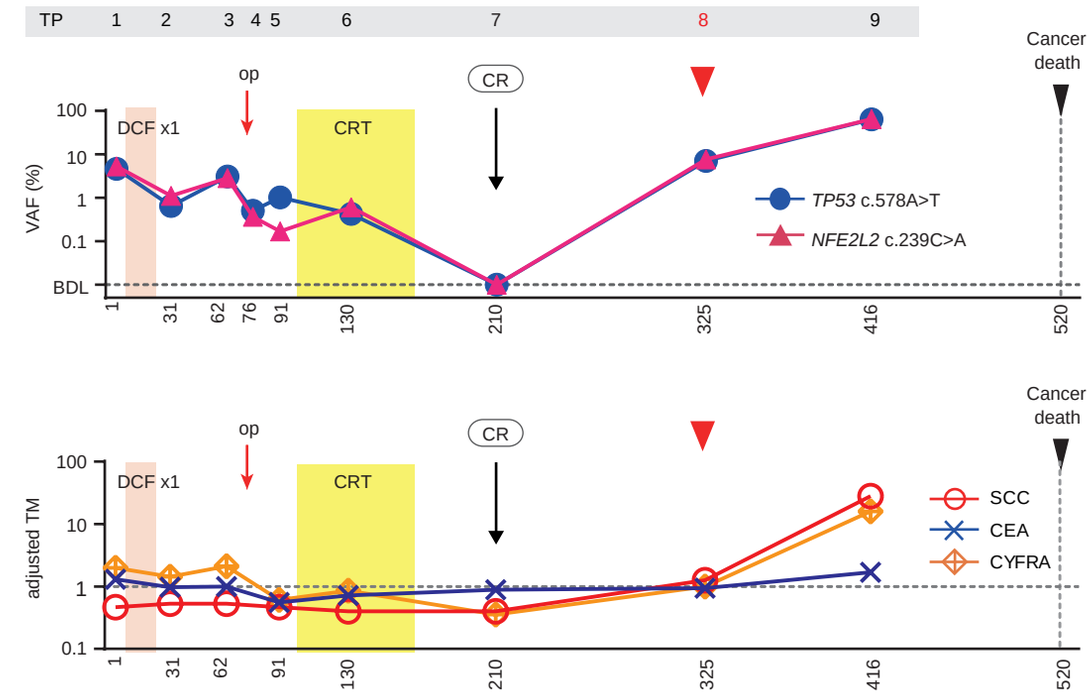

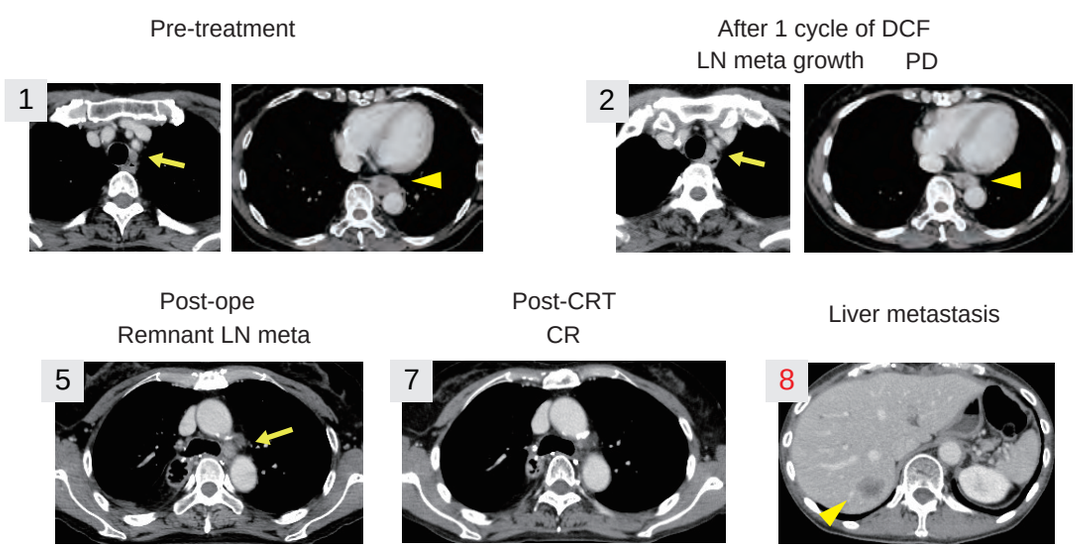

EC_16 had a primary ESCC with adventitia invasion in the middle thoracic esophagus and left recurrent nerve lymph node metastasis (TP 1). After the first cycle of DCF, lymph node metastasis showed growth (TP 2) and subsequent surgical resection was undertaken. A remnant left tracheobronchial lymph node was noted after surgery (TP 5). CRT for mediastinal metastasis was performed and this lesion disappeared (TP 7). Liver metastasis was observed (TP 8) and the patient died of cancer on Day 520. Red arrowheads in the upper panels indicate the time point when recurrence was clinically evident. Arrowheads in CT images indicate primary tumor and liver metastasis whereas arrows indicate lymph node metastasis.

EC_17 Stage IIIA

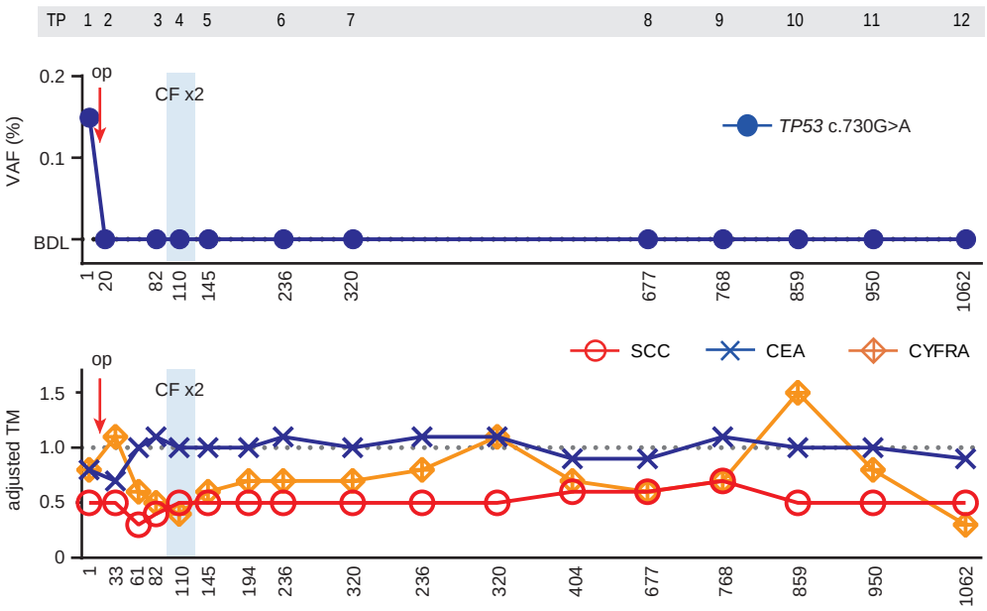

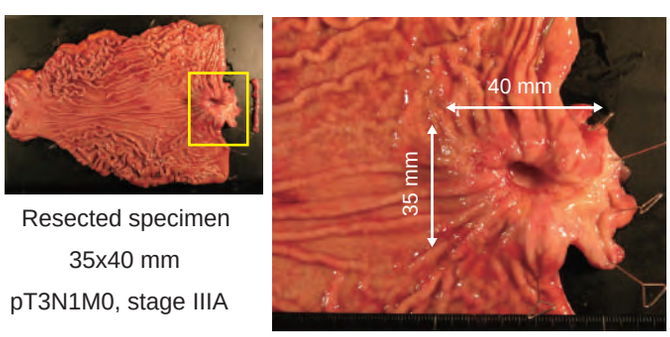

Resected specimen
35x40 mm
pT3N1M0, stage IIIA

EC_17 had a primary ESCC with adventitia invasion in the gastroesophageal junction. Surgical resection was performed as the first line therapy. Microscopically, 2 metastatic nodes were observed as paracardial lymph nodes. This case was diagnosed pathological T3N1M0, stage III. Two cycles of post-operative adjuvant CF therapy were performed. Recurrence was not observed until Day 1,062

EC_18 Stage IV

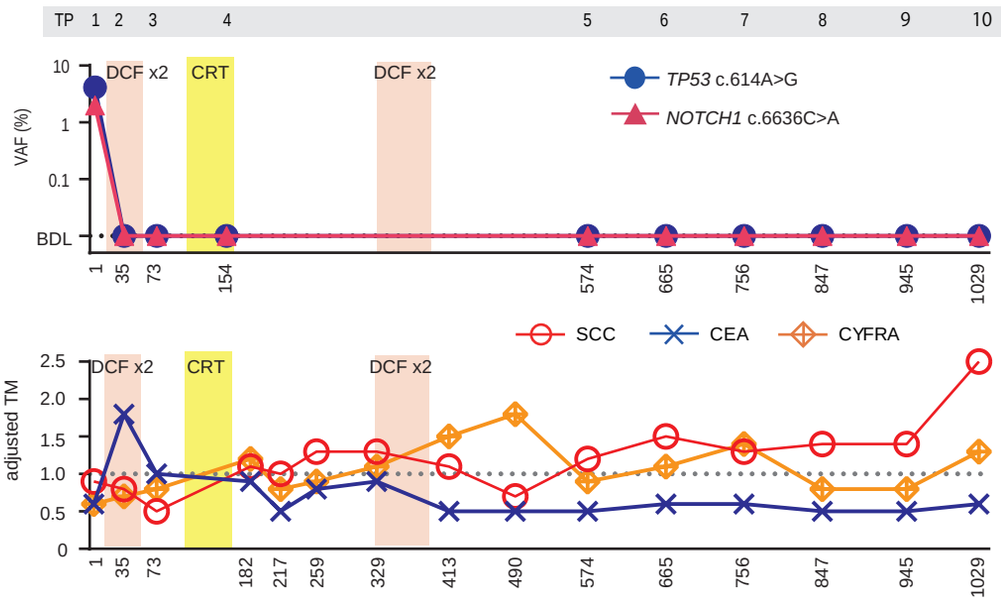

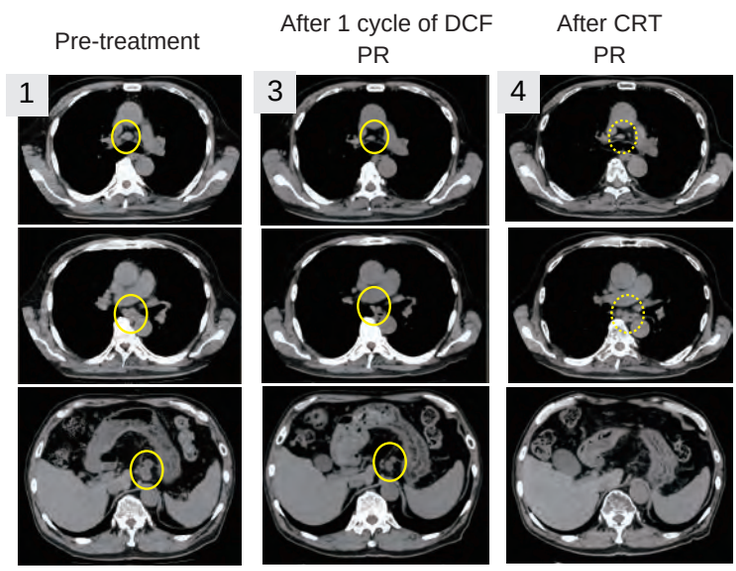

EC_18 had a primary ESCC with submucosal invasion in the lower third of the esophagus and extensive lymph node metastasis. The middle thoracic esophagus was surrounded by multiple enlarged metastatic mediastinal lymph nodes. Extra-regional lymph node metastasis was observed in the pre-tracheal region. Furthermore, metastases were observed in lymph nodes as well as on the left gastric artery and celiac artery (TP 1). This case was diagnosed T1N2M1, Stage IV. Although some mediastinal lymph nodes were still detected after CRT, they were considered to be non-specific lymph node swelling. Recurrence of primary tumor, regrowth lymph node metastasis and emergence of new lesions were not observed through Day 1,029. Yellow circles in CT images indicate primary tumor and lymph node metastasis. Dashed yellow circles indicate mediastinal lymph nodes that were recognized as non-specific findings.

EC_19 Stage IIIC

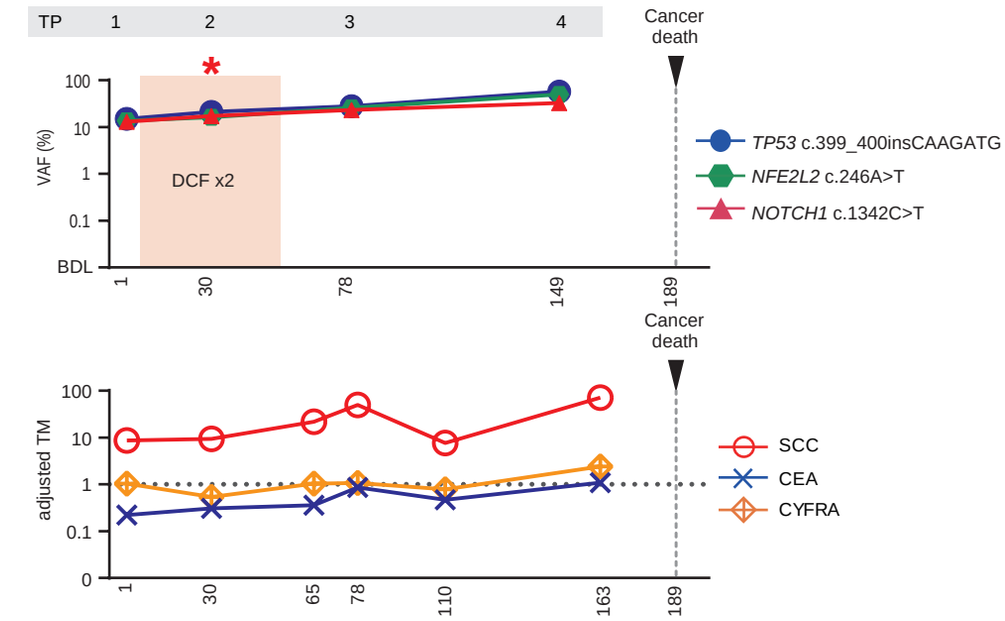

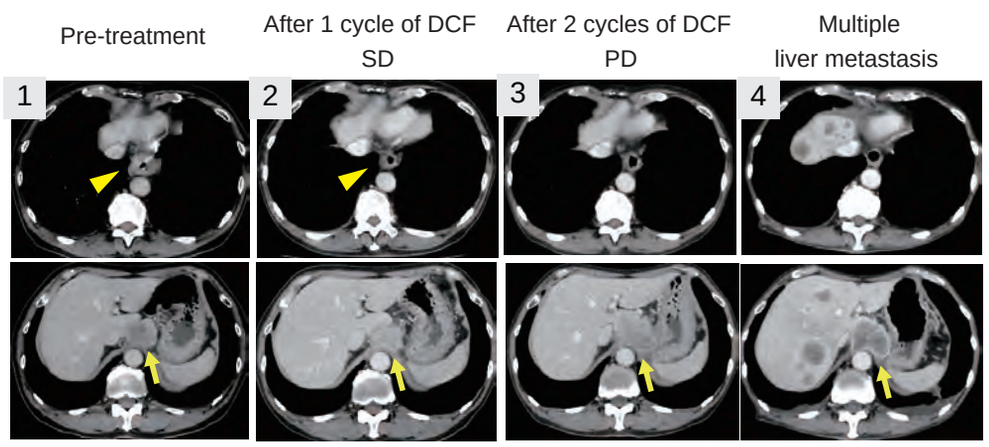

EC_19 had a primary ESCC with adventitia invasion in the lower thoracic esophagus with a bulky abdominal lymph node metastasis (TP 1). After the first cycle of DCF, the response was SD (TP 2). After the second cycle of DCF, the enlarged lymph node metastasis confirmed PD (TP 3). Multiple liver metastases were observed on Day 149 (TP 4), and the patient died on Day 189 after treatment initiation. Asterisks indicate early elevation of ctDNA before tumor growth was confirmed by CT. Arrowheads and arrows in CT images indicate primary tumor and abdominal lymph node metastasis, respectively.

EC_21 Stage IIA

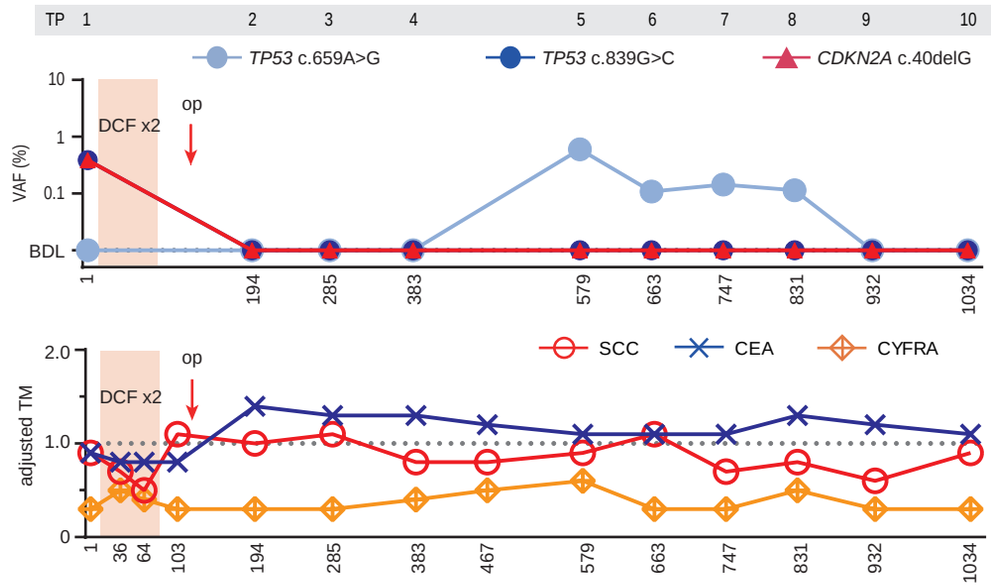

Pre-treatment

Post DCF-2
SD

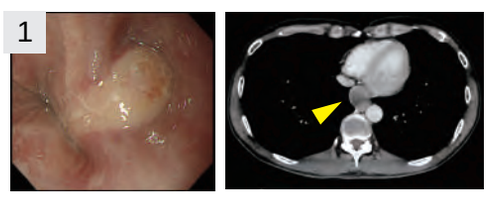

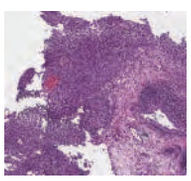

biopsy specimen

squamous cell carcinoma

Resected specimen

leiomyosarcoma, 33x16x25 mm

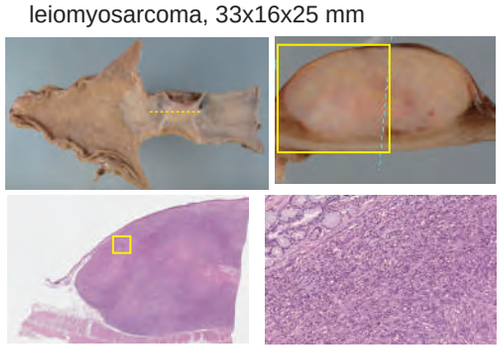

Mediastinal lymph node swelling

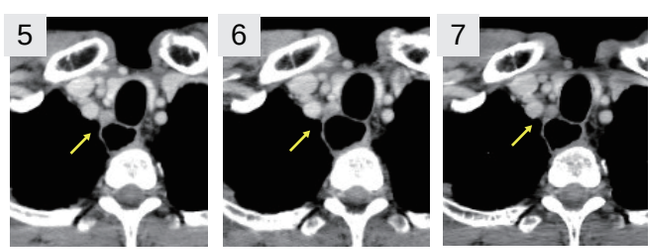

Lymph node metastasis
was not confirmed.

EC_21 had a primary ESCC with adventitia invasion in the lower third of the esophagus (TP 1). This case was clinically diagnosed T3N0M0, Stage IIA ESCC according to CT and biopsy findings. After the second cycle of DCF, the response was SD. Surgical resection was subsequently performed. Microscopically, the remnant esophageal tumor was classified as leiomyosarcoma comprising malignant spindle cells. According to the pathological findings in the pretreatment biopsy specimen and resected specimen, the tumor was diagnosed as carcinosarcoma. No recurrence has been observed through Day 1,034. Arrowheads in CT images indicate primary tumor, whereas arrows indicate right recurrent nerve lymph node swelling.

EC_22 Stage IIB

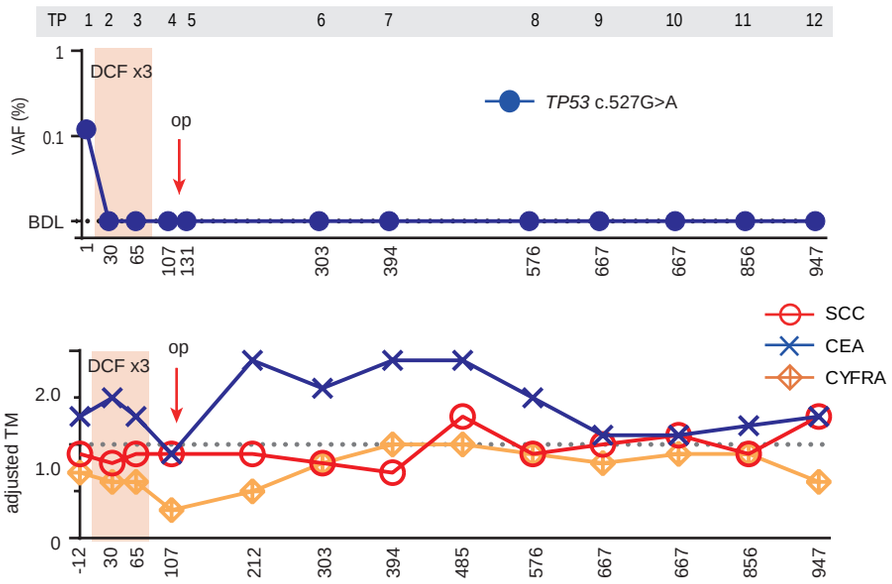

Pre-treatment

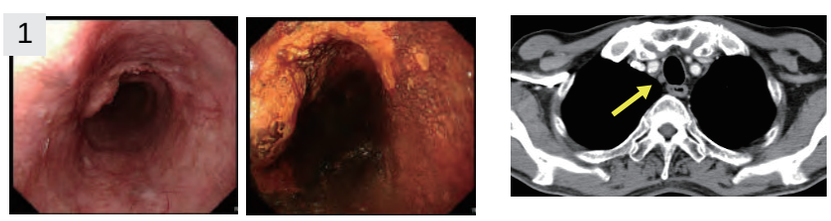

Resected specimen 2 x 2 mm^2, pTisN0M0, Stage 0

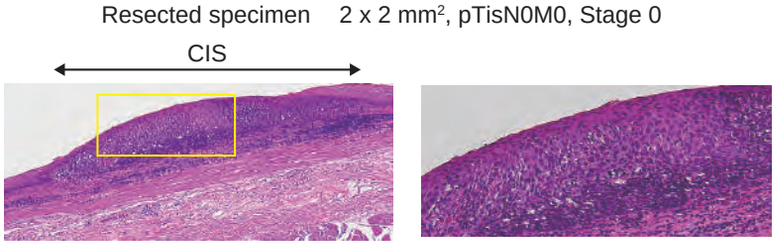

EC_22 had a primary ESCC with muscular layer invasion in the middle third of the esophagus and right recurrent nerve lymph node metastasis (TP 1, pretreatment endoscopic (left) and CT (right) images are shown). At the end of the third cycle of DCF, surgical resection was performed. Remnant cancer cells were limited to the esophageal epithelium layer in a 2 x 2 mm^2 area. Recurrence was not observed until Day 947. Arrow in the CT image indicates right recurrent nerve lymph node metastasis.

EC_23 Stage IA

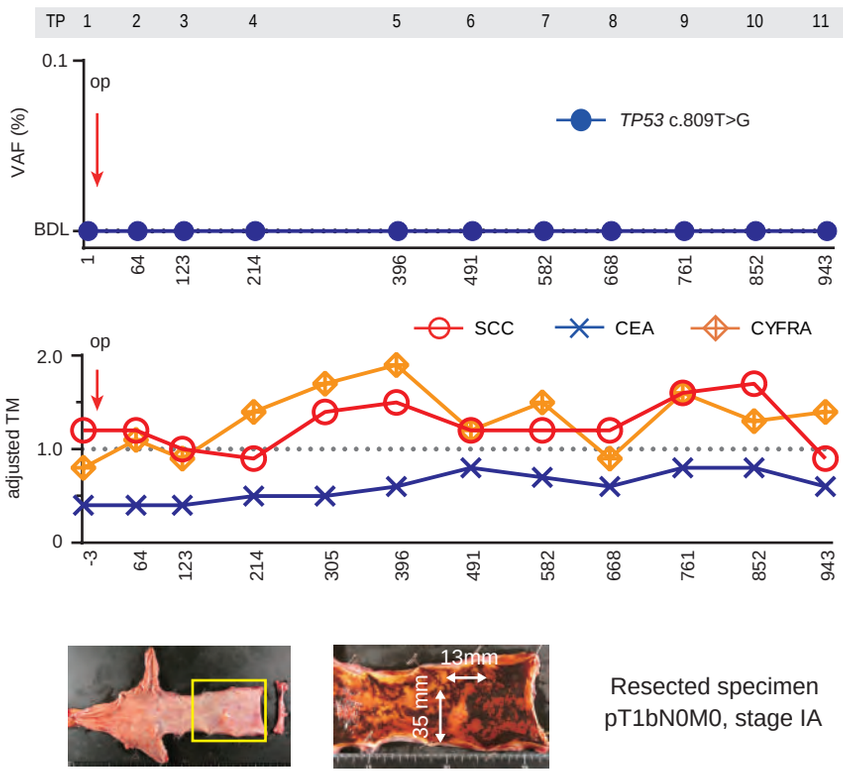

Resected specimen
pT1bN0M0, stage IA

EC_23 had superficial ESCC in the middle third of the esophagus. Although areas of the resected specimen lacking Lugol' s staining were frequently observed throughout the esophagus, the area of cancer was limited to 13 x 35 mm^2 (enlarged image). Microscopic pathological examinations revealed that tumor invasion was limited to the submucosal layer. Lymph node metastasis was not observed.

EC_24 Stage IIIC

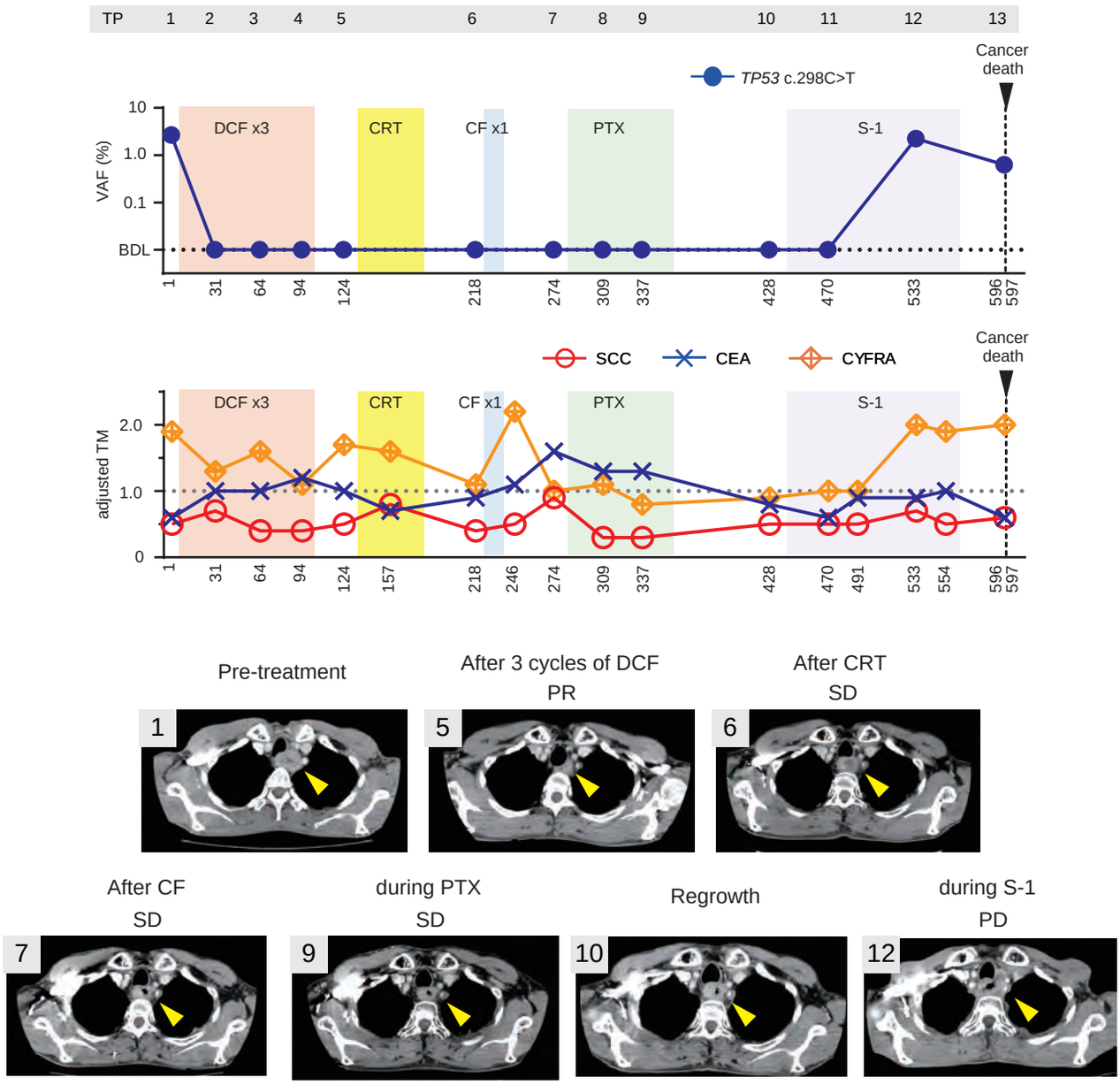

EC_24 had a primary ESCC with trachea invasion in the cervical esophagus (TP 1). This case was diagnosed T4bN0M0, Stage IIIC. After the third cycle of DCF, tumor reduction was observed (TP 5). As cervical esophageal edema and stenosis remained after CRT, chemotherapies with CF, PTX, and S-1 continued. Although thickening of the cervical esophagus wall was persistently observed, new lesions and tumor regrowth were not evident until Day 428. The patient died of cancer progression on Day 597. Arrowheads indicate the main tumor.

EC_25 Stage IIIA

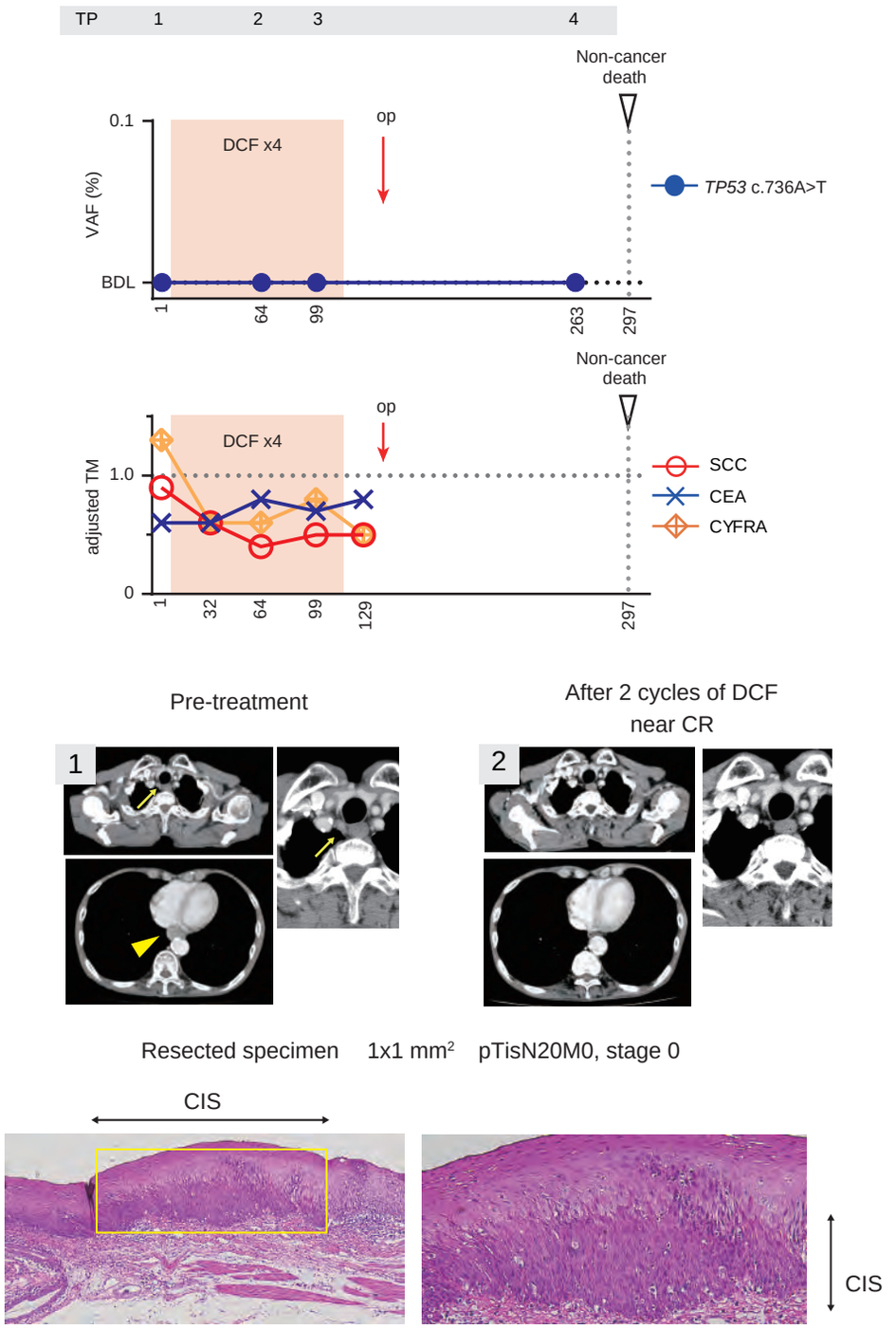

EC_25 had a primary ESCC with adventitia invasion in the lower third of the esophagus and a right recurrent nerve lymph node metastasis (TP 1). This case was diagnosed T3N1M0, Stage IIIA. At the end of the second cycle of DCF, remarkable tumor shrinkage was observed in both the primary tumor and the metastatic node (TP 2). In the resected specimen, remnant cancer cells were limited to the epithelial layer in a 1.0 x1.0 mm^2 area. The area of carcinoma in situ (CIS) is shown in microscopy figures. VAF of mutations detected in the pre-treatment primary tumor were all <5 % by NGS analysis (eTable 3). Arrowhead and arrows indicate primary tumor and lymph node metastasis, respectively.

EC_26 Stage IIIC

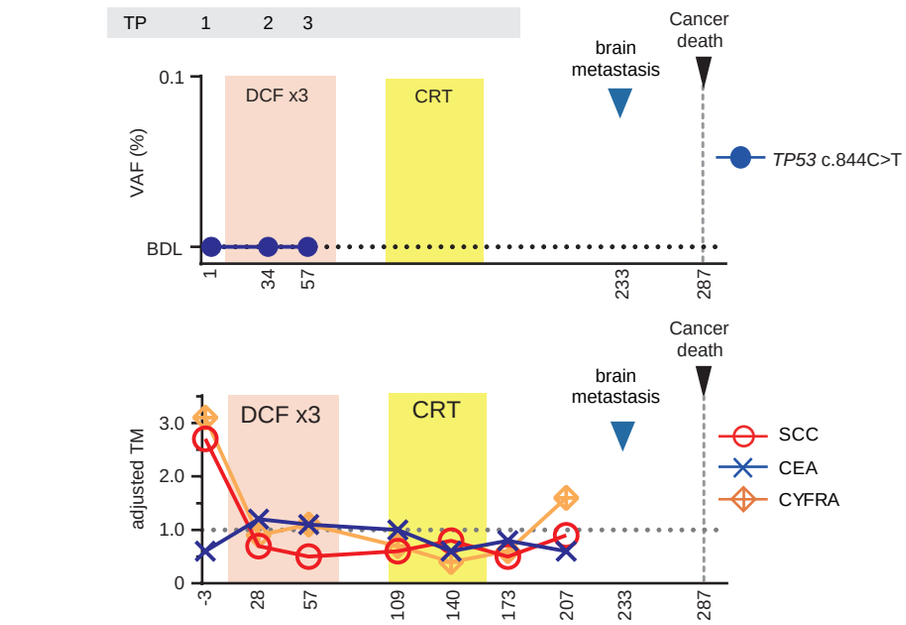

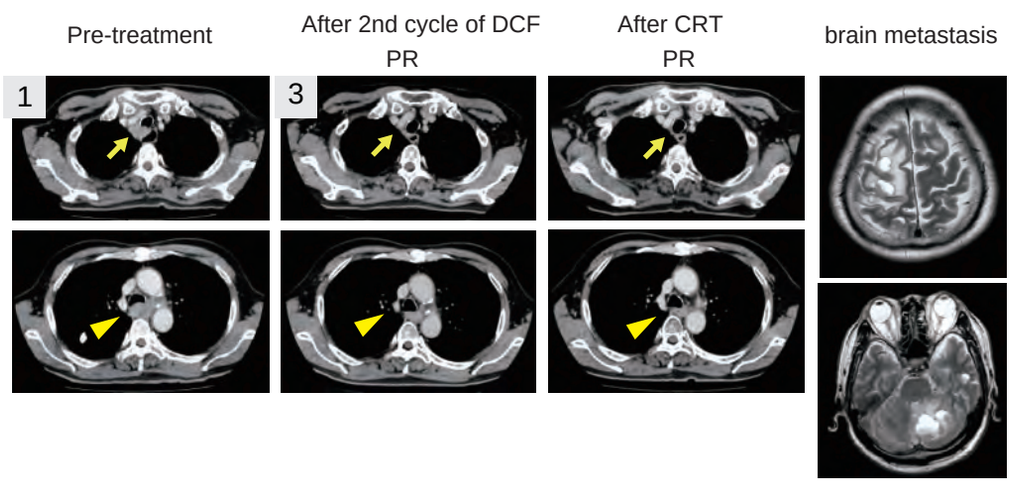

EC_26 had a primary ESCC with trachea invasion in the middle third of the esophagus. A lymph node metastasis at the right recurrent nerve and tracheal invasion (TP 1) were found. This case was diagnosed T4bN1M0, Stage IIIC. After the third cycle of DCF, shrinkage of the primary tumor and lymph node metastasis were observed. A CRT with curative intent was subsequently initiated. Tumor shrinkage was sustained after CRT, and the patient was referred to a local hospital for subsequent chemotherapy. Multiple brain metastases were observed on Day 233 and the patient died of cancer on Day 287. Arrowheads and arrows in CT images indicate primary tumor and lymph node metastasis, respectively.

EC_28 Stage IA

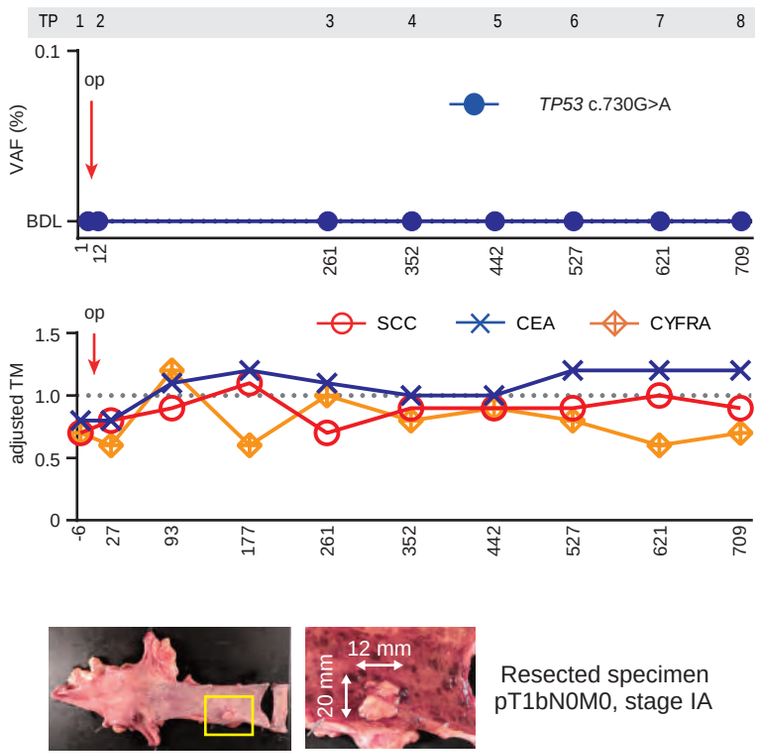

Resected specimen
pT1bN0M0, stage IA

EC_28 had superficial ESCC in the middle third of the esophagus. The tumor was 12 x 20 mm^2 and areas unstained with Lugol and tumor invasion were limited to the submucosal layer upon microscopic examination. Lymph node metastasis was not observed.

EC_29 Stage IIIC

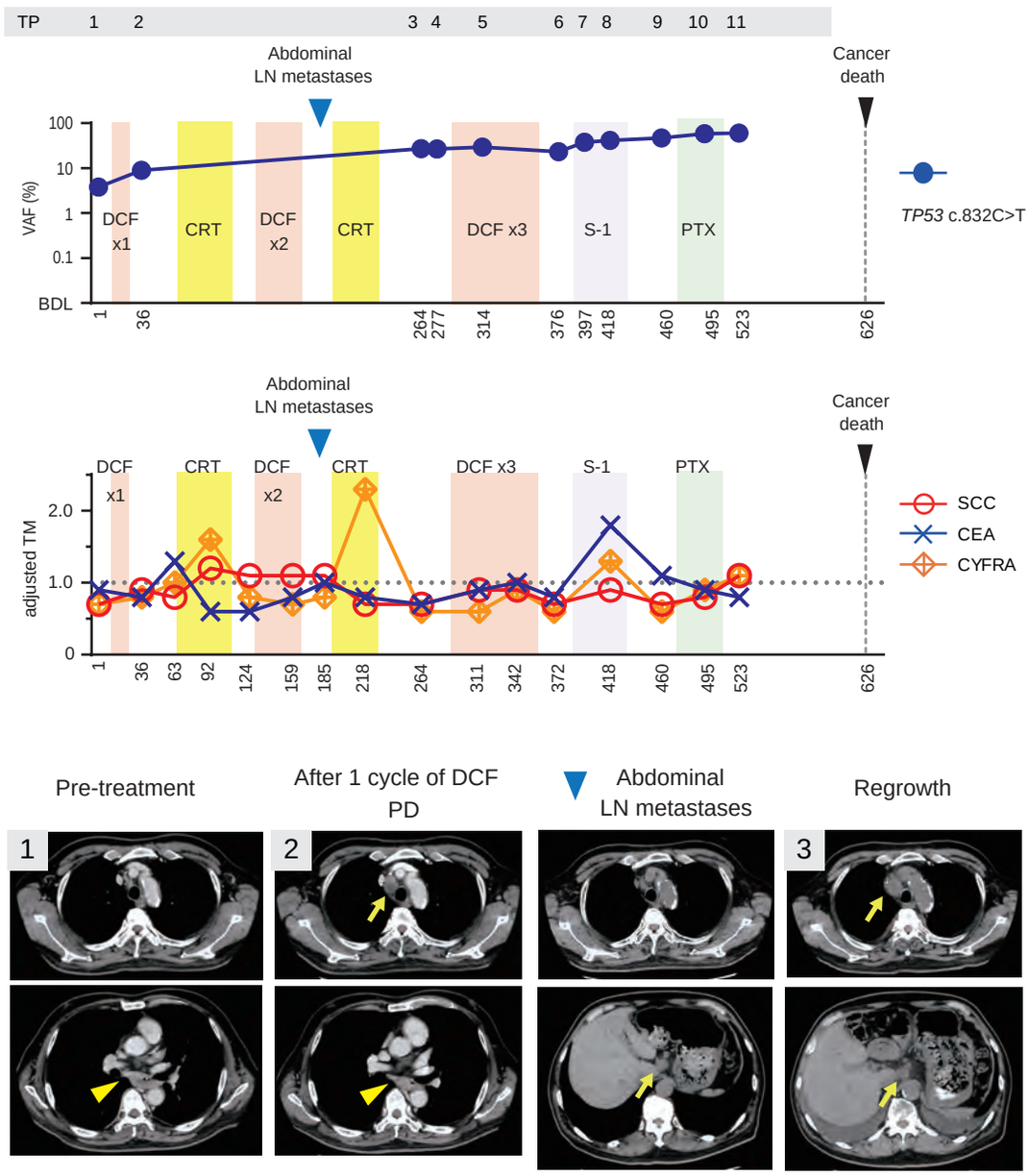

EC_29 had a primary ESCC with left main bronchus and thoracic aorta invasion in the middle third of the esophagus, as well as the right recurrent nerve. Middle and lower para-esophageal lymph nodes metastases were also seen (TP 1). This case was diagnosed T4bN2M0, Stage IIIC. As enlargement of the right recurrent nerve lymph node metastasis was observed after the first cycle of DCF (TP 2), CRT for the primary tumor and mediastinal lymph nodes followed by 2 cycles of DCF was performed. Although primary tumor and mediastinal lymph nodes were reduced after the first CRT, paracardial and lesser curvature lymph node metastases along the branches of the left gastric artery were evident. A second cycle of CRT for the abdominal lymph nodes was performed but no reduction in tumor volume was achieved (TP 3). An additional three cycles of DCF, oral S-1 administration, and weekly paclitaxel therapy continued with no response. The patient died of cancer progression on Day 626. Arrowheads and arrows indicate primary tumor and lymph node metastasis, respectively.

EC_30 Stage IIIB

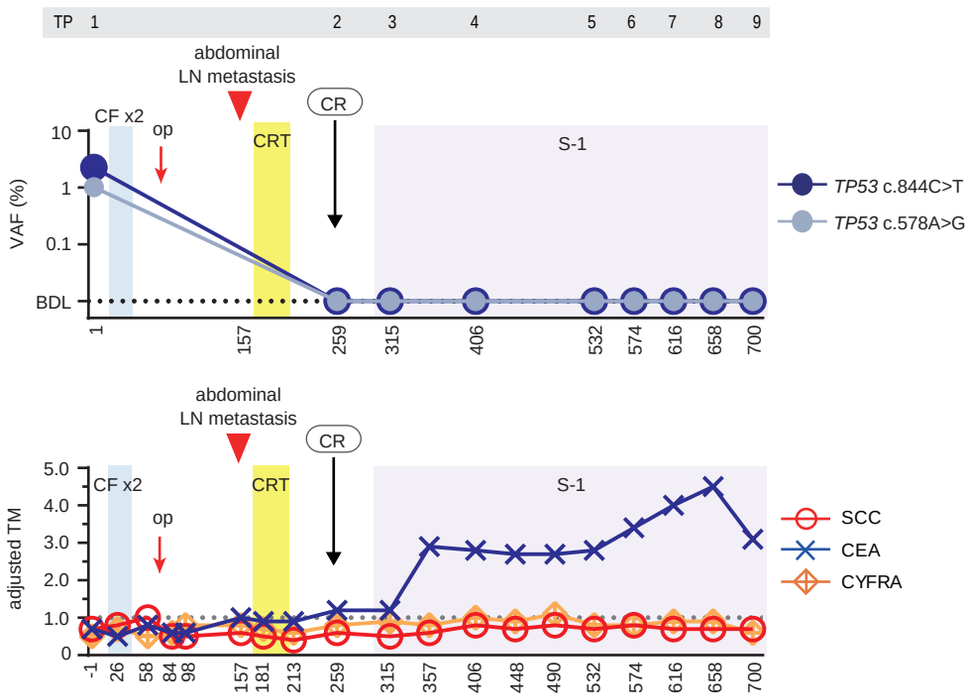

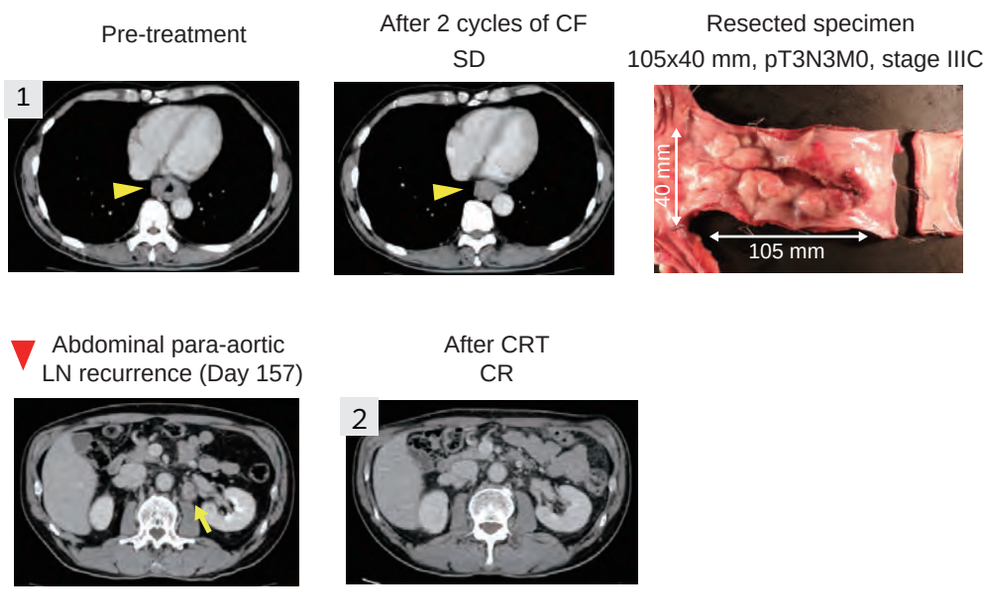

EC_30 had a primary ESCC with adventitia invasion in the middle and lower third of the esophagus, and bulky lesser curvature lymph node metastases to the stomach as well as branches of the left gastric artery, and the right recurrent nerve. This case was diagnosed T3N2M0, Stage IIIB. Tumor shrinkage was not observed after CF and the resected specimen demonstrated a bulky tumor. Microscopically, 13 metastatic nodes were observed in abdominal lymph nodes. On Day 157, abdominal para-aortic lymph node recurrence was noted. Subsequent CRT achieved CR (TP 2), followed by S-1 adjuvant chemotherapy. No recurrence has been observed through Day 700. Arrowheads and arrow indicate primary tumor and lymph node metastasis, respectively.

EC_31 Stage IA

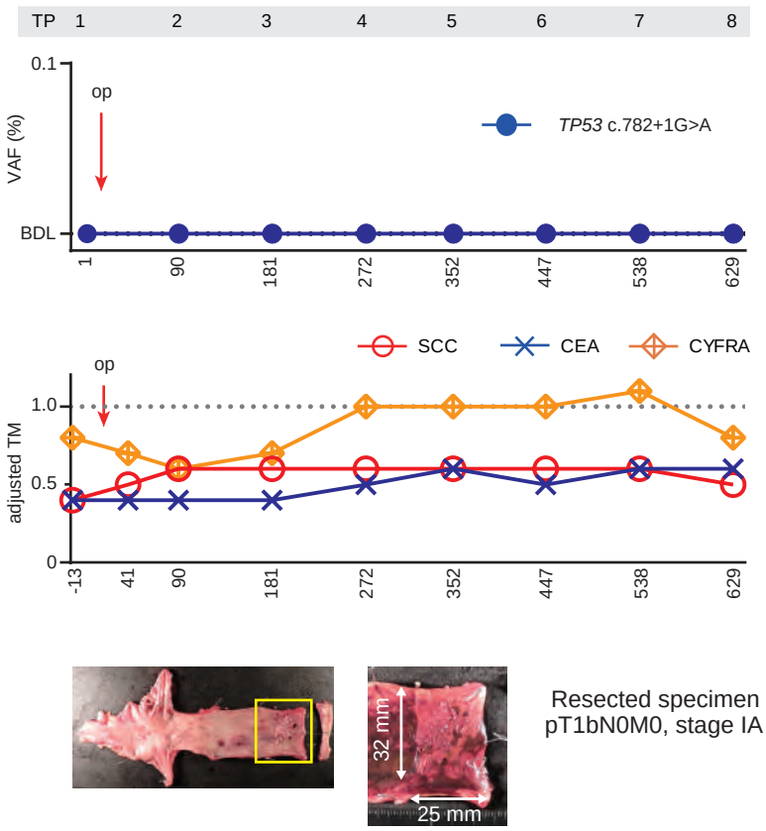

Resected specimen
pT1bN0M0, stage IA

EC_31 had superficial ESCC in the upper third of the esophagus. Macroscopic images of the resected specimen revealed that tumor had an area of 25 x 32 mm^2 that was unstained by Lugol. Pathological examination showed that tumor invasion was limited to the submucosal layer.

EC_32 Stage IIIC

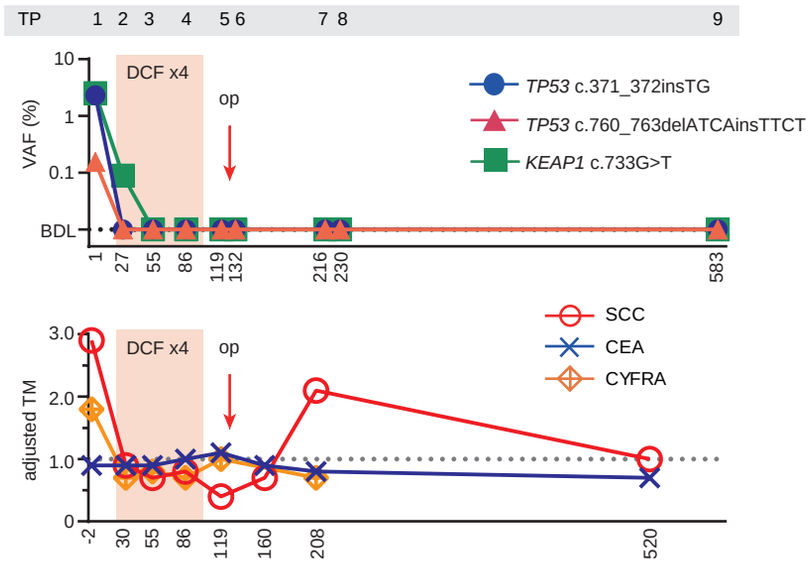

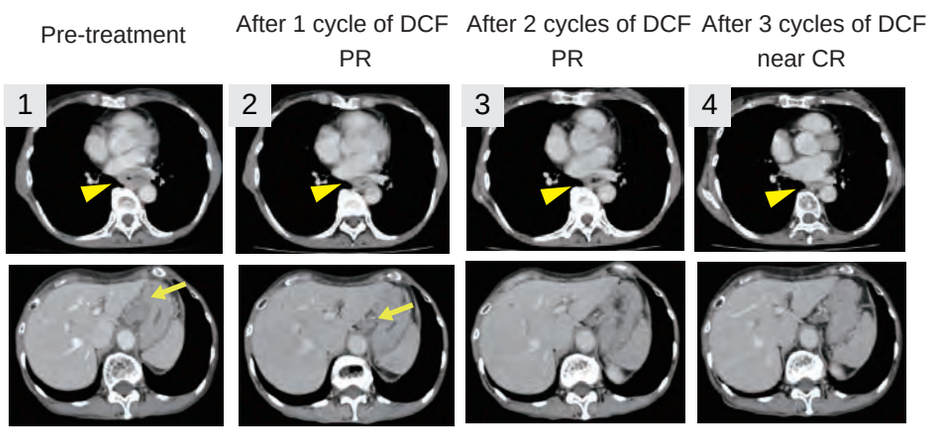

Resected specimen 15 x 4 mm^2, pT1aN1M0, stage IB

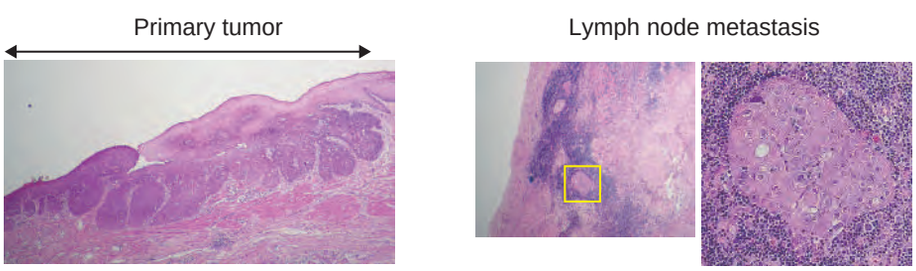

EC_32 had a primary ESCC with adjacent pleural and pericardium invasion in the middle third of the esophagus and bulky lesser curvature lymph node metastases to the stomach as well as branches of the left gastric artery (TP 1). This case was diagnosed T4aN1M0, Stage IIIC. After the fourth cycle of DCF, remarkable tumor shrinkage was observed and surgical resection was performed. In the resected specimen, remnant cancer cells were limited to the muscularis mucosa in a 15 x 4 mm^2 area in the esophagus and a small area in the lesser curvature lymph node metastasis that had extensive fibrosis. Recurrence has not been observed through Day 520. Arrowheads and arrows in CT images indicate primary tumor and lymph node metastasis, respectively.

EC_33 Stage IIIC

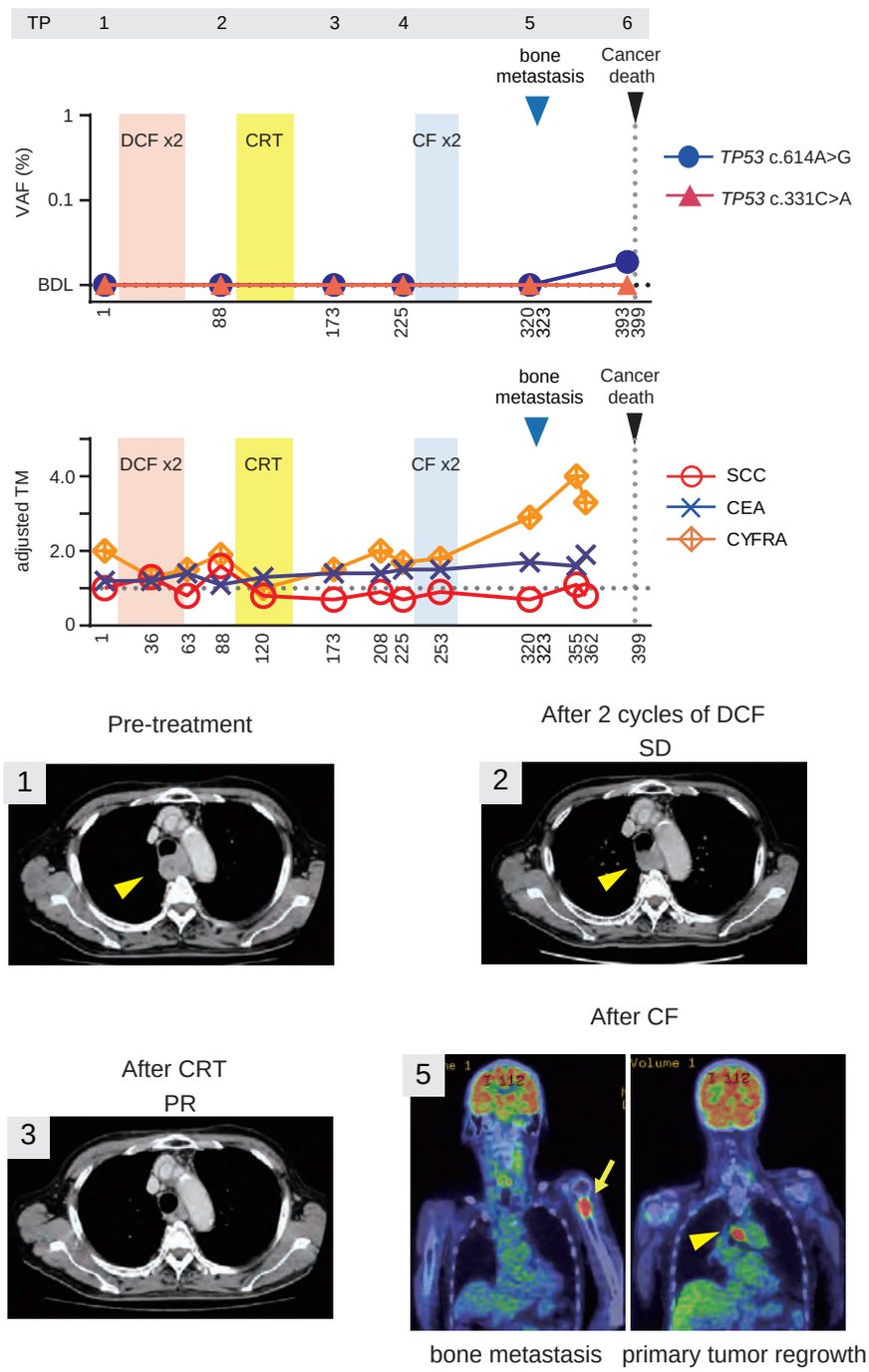

EC_33 had a primary ESCC with trachea invasion in the upper third of the esophagus and a right recurrent nerve lymph node metastasis. This case was diagnosed T4bN1M0, Stage IIIC. Tumor shrinkage was not observed after two cycles of DCF, but the tumor was reduced after CRT and the patient had a PR (TP 2 and 3). After two cycles of CF, by Day 323 bone metastasis in the left humerus and primary tumor regrowth were observed by FDG-PET/CT. The patient died of cancer on Day 399. Arrowheads and arrow indicate primary tumor and bone metastasis, respectively.

EC_34 Stage IA

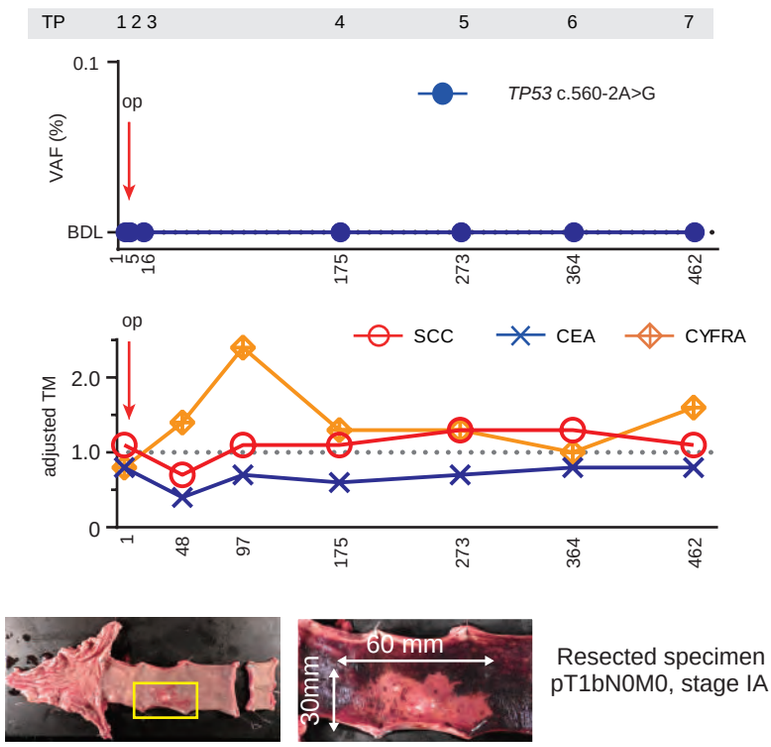

Resected specimen
pT1bN0M0, stage IA

EC_34 had a superficial ESCC in the lower third of the esophagus. The resected tumor had a 60 x 30 mm^2 area that was unstained by Lugol. Pathological examination revealed that tumor invasion was limited to the submucosal layer.

EC_35 Stage IIIC

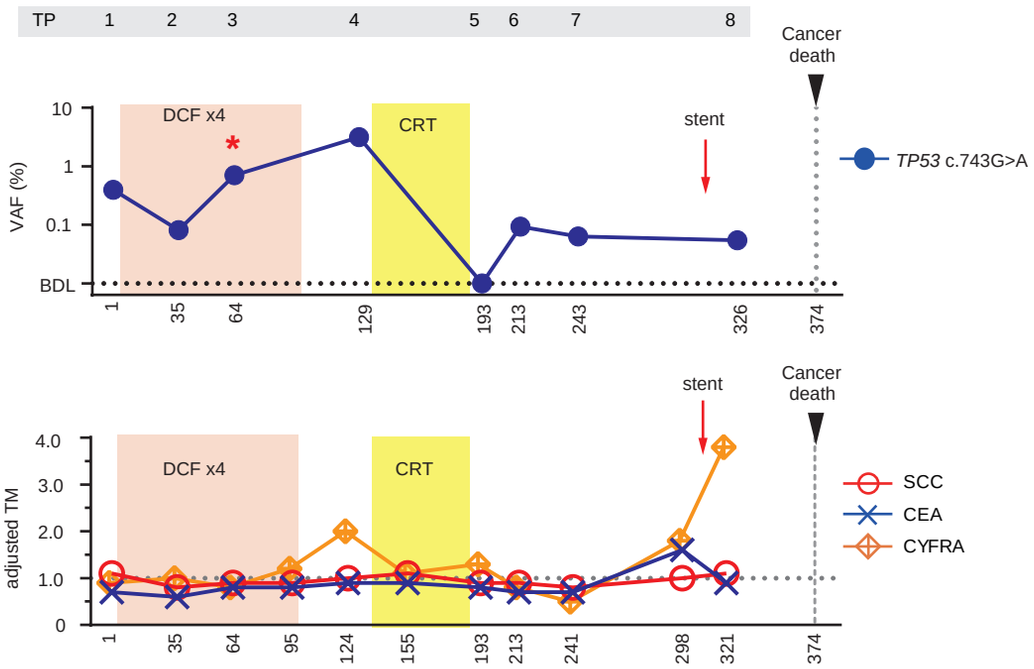

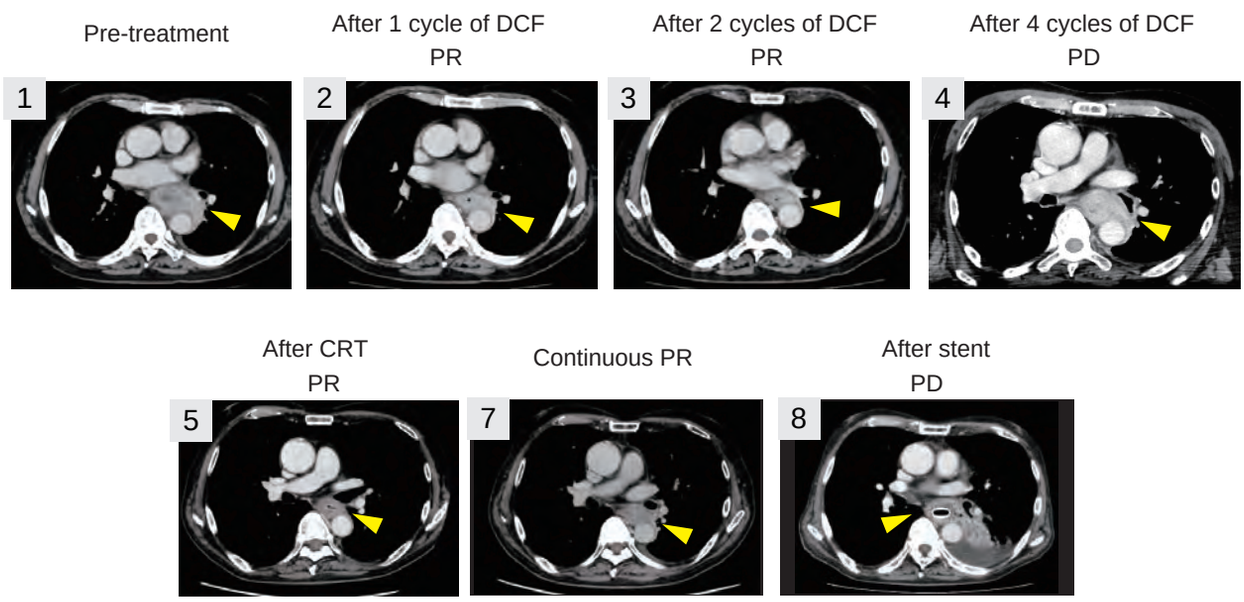

EC_35 had a bulky primary ESCC that invaded the thoracic aorta in the middle third of the esophagus (TP 1). After the first cycle of DCF, tumor shrinkage was observed, but by the end of the fourth cycle of DCF, tumor regrowth was observed (TP 4). A CRT showed remarkable, temporary shrinkage of the primary tumor (TP 5), but esophageal stenosis progressed (TP 6-8). An esophageal stent was inserted. The patient died of cancer on Day 374. Asterisks indicate early elevation of ctDNA before tumor regrowth was confirmed by CT. Arrowheads indicate primary tumor.

EC_36 Stage IB

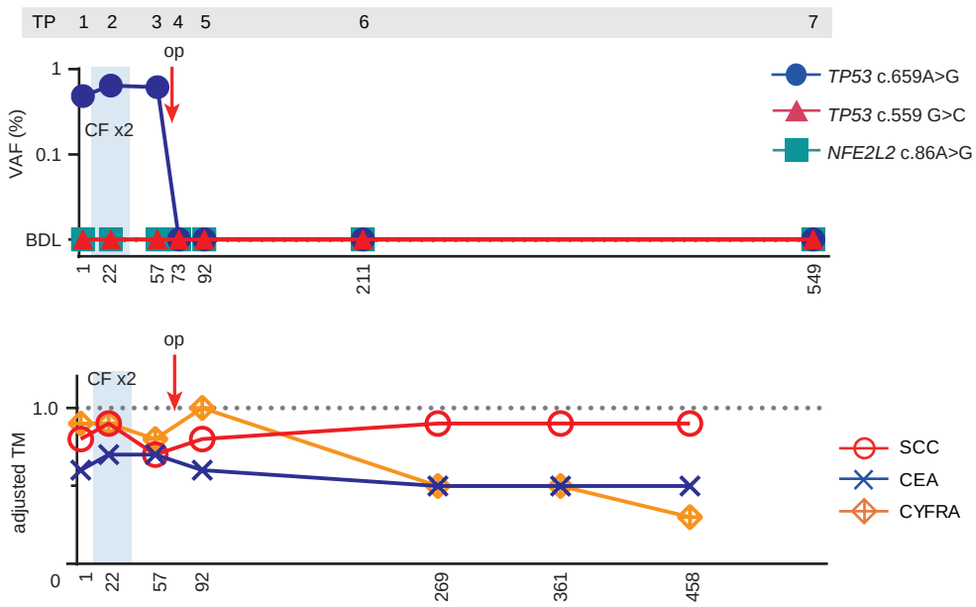

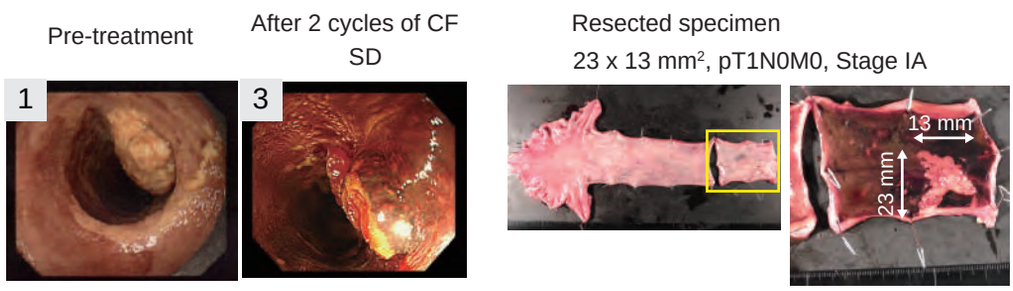

EC_36 had a primary ESCC with muscular invasion in the upper third of the esophagus. This case was diagnosed T2N0M0, Stage IB. Endoscopic images of the primary tumor at pre-treatment (TP 1) and after CF (TP 3) are shown. In the resected specimen, the tumor had a 13 x 23 mm² area that was not stained by Lugol. Pathological examination indicated that remnant cancer cells were limited to the submucosal layer. No recurrence was observed after surgery through Day 549.